








## ORIGINAL RESEARCH

# Myosin Light Chain Phosphatase Plays an Important Role in Cardiac Fibrosis in a Model of Mineralocorticoid Receptor-Associated Hypertension

Zhe Ye, MD; Ryuji Okamoto , MD, PhD; Hiromasa Ito, MD, PhD; Rie Ito, BScAgr; Keishi Moriwaki , MD, PhD; Mizuki Ichikawa, MD; Lupiya Kimena , MD; Yusuf Ali , PhD; Masaaki Ito , MD, PhD; Celso E. Gomez-Sanchez , MD; Kaoru Dohi , MD, PhD

**BACKGROUND:** Myosin phosphatase targeting subunit 2 (MYPT2) is an important subunit of cardiac MLC (myosin light chain) phosphatase, which plays a crucial role in regulating the phosphorylation of MLC to phospho-MLC (p-MLC). A recent study demonstrated mineralocorticoid receptor-related hypertension is associated with RhoA/Rho-associated kinase/MYPT1 signaling upregulation in smooth muscle cells. Our purpose is to investigate the effect of MYPT2 on cardiac function and fibrosis in mineralocorticoid receptor-related hypertension.

**METHODS AND RESULTS:** HL-1 murine cardiomyocytes were incubated with different concentrations or durations of aldosterone. After 24-hour stimulation, aldosterone increased CTGF (connective tissue growth factor) and MYPT2 and decreased p-MLC in a dose-dependent manner. MYPT2 knockdown decreased CTGF. Cardiac-specific MYPT2-knockout (c-MYPT2<sup>-/-</sup>) mice exhibited decreased type 1 phosphatase catalytic subunit  $\beta$  and increased p-MLC. A disease model of mouse was induced by subcutaneous aldosterone and 8% NaCl food for 4 weeks after uninephrectomy. Blood pressure elevation and left ventricular hypertrophy were observed in both c-MYPT2<sup>-/-</sup> and MYPT2<sup>+/+</sup> mice, with no difference in heart weights or nuclear localization of mineralocorticoid receptor in cardiomyocytes. However, c-MYPT2<sup>-/-</sup> mice had higher ejection fraction and fractional shortening on echocardiography after aldosterone treatment. Histopathology revealed less fibrosis, reduced CTGF, and increased p-MLC in c-MYPT2<sup>-/-</sup> mice. Basal global radial strain and global longitudinal strain were higher in c-MYPT2<sup>-/-</sup> than in MYPT2<sup>+/+</sup> mice. After aldosterone treatment, both global radial strain and global longitudinal strain remained higher in c-MYPT2<sup>-/-</sup> mice compared with MYPT2<sup>+/+</sup> mice.

**CONCLUSIONS:** Cardiac-specific MYPT2 knockout leads to decreased myosin light chain phosphatase and increased p-MLC. MYPT2 deletion prevented cardiac fibrosis and dysfunction in a model of mineralocorticoid receptor-associated hypertension.

**Key Words:** aldosterone ■ cardiac fibrosis ■ mineralocorticoid receptor ■ myosin light chain ■ phosphorylation

**M**ineralocorticoid receptor (MR) is an important receptor through which aldosterone, cortisol, and mechanical stimulation can lead to organ fibrosis and hypertension.<sup>1</sup> Primary aldosteronism is seen in 5% to 10% of patients with hypertension and represents the most common form of secondary hypertension.<sup>2</sup> The risk of hypertensive organ damage, including heart failure, is much higher (2.0-fold)

Correspondence to: Ryuji Okamoto, MD, PhD, Department of Cardiology and Nephrology, Mie University Graduate School of Medicine, 2-174 Edobashi, Tsu, Mie 514-8507, Japan. Email: [ryuji@clin.medic.mie-u.ac.jp](mailto:ryuji@clin.medic.mie-u.ac.jp)

This work was presented in part at the European Society of Cardiology Congress, August 25–28, 2023, in Amsterdam, Netherlands, and presented in part at the American Heart Association Scientific Sessions, November 11–13, 2023, in Philadelphia, PA.

This article was sent to Julie K. Freed, MD, PhD, Associate Editor, for review by expert referees, editorial decision, and final disposition.

Supplemental Material is available at <https://www.ahajournals.org/doi/suppl/10.1161/JAHA.123.032828>

For Sources of Funding and Disclosures, see page 14.

© 2024 The Authors. Published on behalf of the American Heart Association, Inc., by Wiley. This is an open access article under the terms of the [Creative Commons Attribution-NonCommercial-NoDerivs](https://creativecommons.org/licenses/by-nc-nd/4.0/) License, which permits use and distribution in any medium, provided the original work is properly cited, the use is non-commercial and no modifications or adaptations are made.

JAHA is available at: [www.ahajournals.org/journal/jaha](http://www.ahajournals.org/journal/jaha)

## RESEARCH PERSPECTIVE

### What Is New?

- Aldosterone induced the expression of myosin phosphatase target subunit 2 and the decrease in the level of p-MLC (phosphorylation of ventricular myosin light chain) in HL-1 cardiomyocytes and mice hearts.
- Myosin phosphatase target subunit 2 knockout prevented cardiac fibrosis induced by aldosterone partly due to the increase in the level of p-MLC and the attenuation of connective tissue growth factor expression.

### What Question Should Be Addressed Next?

- Our results indicated that myosin phosphatase target subunit 2 may be a potential target for preventing cardiac fibrosis and dysfunction in a model of mineralocorticoid receptor-associated hypertension, and the studies on the upstream and downstream regulation of myosin phosphatase target subunit 2 and the association of mineralocorticoid receptor are important for future clinical studies.

## Nonstandard Abbreviations and Acronyms

<b>c-MYPT2<sup>-/-</sup></b>	cardiac-specific MYPT2-knockout
<b>CTGF</b>	connective tissue growth factor
<b>GLS</b>	global longitudinal strain
<b>GRS</b>	global radial strain
<b>KO</b>	cardiac-specific knockout
<b>MLC</b>	myosin light chain
<b>MLCK</b>	myosin light chain kinase
<b>MLCP</b>	myosin light chain phosphatase
<b>MR</b>	mineralocorticoid receptor
<b>MYPT</b>	myosin phosphatase target subunit
<b>PP1<math>\beta</math></b>	protein phosphatase catalytic subunit beta, also known as PP1c $\delta$
<b>ROCK</b>	Rho kinase
<b>Treated</b>	MR-related hypertension

in patients with primary aldosteronism than in those with equivalent essential hypertension.<sup>3</sup> This is partly attributable to more pronounced left ventricular (LV) remodeling, including cardiac fibrosis induced by MR signaling.<sup>4-7</sup> In addition, cortisol can activate MR and

cause cardiac dysfunction in the patients with pseudoaldosteronism.<sup>8</sup> However, how MR signaling exerts this deleterious influence on cardiac fibrosis remains unclear. In addition, CTGF (connective tissue growth factor) plays an important role in the development of organ fibrosis.<sup>9,10</sup>

Ventricular levels of p-MLC (phosphorylated myosin light chain) could change according to the balance between MLCK (MLC kinase) and MLC phosphatase (MLCP) activities.<sup>11</sup> In end-stage human heart failure, p-MLC levels are significantly lower than in donors.<sup>12</sup> The importance of regulating p-MLC level has recently been highlighted by the fact that mutations in the gene (*MYLK3*) encoding cMLCK (cardiac MLCK) are associated with familial dilated cardiomyopathy.<sup>13,14</sup> Our group and others have previously reported that MLCP transgenic mice<sup>15</sup> and cMLCK-deficient mice<sup>16,17</sup> show increased levels of p-MLC and cardiac dysfunction with LV dilatation in the natural course. The regulation of p-MLC thus seems to play an important role in cardiac function and remodeling.

MR-related hypertension has recently been reported to be associated with the upregulation of ROCK (RhoA/Rho kinase)-myosin phosphatase target subunit 1 (MYPT1) signaling in arteries.<sup>18,19</sup> However, how MYPT signaling affects the heart in MR-related hypertension remains unknown. A recent study demonstrated that cardiac MLCP plays an important role in cardiac fibrosis as a target of ROCK.<sup>20</sup> Cardiac MLCP consists of 3 subunits, including MYPT2, of which isoform MYPT1 is also known as a myosin-binding subunit.<sup>21</sup> MYPT2 can directly interact with RhoA and increase phosphatase activity 11-fold, with cardiac MLC as a substrate.<sup>22</sup>

How the loss of MYPT2 affects cardiac function and fibrosis in MR-related hypertension remains unclear. Our purpose is to investigate the effect of MYPT2 on cardiac function and fibrosis in MR-related hypertension. We developed a model of MR-related cardiac fibrosis using mice with cardiac-specific knockout (KO) of MYPT2 and aldosterone treatment after uninephrectomy.<sup>23</sup> We also evaluated the effects of MYPT2 deletion on CTGF expression.

## METHODS

The authors declare that all supporting data are available within the article, including the Supplemental Material.

## Cell Culture and Drug Treatments

The HL-1 cardiac muscle cell line was purchased and cultured according to the protocol of the supplier (Merck Millipore, Burlington, MA). HL-1 can be serially passaged while maintaining the ability to contract and retaining differentiated cardiac morphological,

biochemical, and electrophysiological properties.<sup>24</sup> Cardiomyocytes plated in flasks coated with fibronectin (F-1141; Sigma-Aldrich, Irvine, CA)-gelatin (F-1141; Sigma-Aldrich) were maintained in Complete Claycomb Medium (51800C; Sigma-Aldrich) supplemented with 100  $\mu$ mol/L norepinephrine (A0937; Sigma-Aldrich), 100 U/mL penicillin (Sigma-Aldrich), 100  $\mu$ g/mL streptomycin (Sigma-Aldrich), 2 mmol/L L-glutamine (Sigma-Aldrich), and 10% HL-1 qualified fetal bovine serum (TMS-016-B; Merck Millipore) in a humidified 5% CO<sub>2</sub> incubator at 37 °C in accordance with the protocol recommended by the manufacturer. Medium was routinely replaced every 24 hours. After serum starvation for 24 hours, cells were treated with aldosterone (10<sup>-5</sup>, 10<sup>-6</sup>, or 10<sup>-7</sup> mol/L) and subsequently harvested after 1 or 24 hours. The stock solution of aldosterone (aldosterone powder, 1 mg/mL; Sigma-Aldrich) was prepared by addition of dimethyl sulfoxide (Nacalai Tesque, Kyoto, Japan), vortexing until dissolved, and storing at -20 °C until use.

### Western Blotting

Mouse hearts were individually homogenized in ice-cold radio-immunoprecipitation assay buffer and 1 $\times$  protease inhibitor mixture (Roche, Basel, Switzerland). Samples were separated on SDS-PAGE (10% or 12.5% gel) and transferred to a polyvinylidene fluoride membrane. This membrane was then blocked for 1 hour and probed overnight with our previously generated primary antibodies (against MYPT2,<sup>22</sup> leucine zipper,<sup>22</sup> PP1 $\beta$  [beta catalytic subunit of protein phosphatase 1, also known as PP1c $\delta$ ],<sup>25</sup> cMLCK1 and 2<sup>16</sup>) in 1% nonfat dry milk at 4 °C. Leucine zipper antibody can recognize MYPT2, MYPT1, and heart-specific small regulatory subunit of MLCP simultaneously.<sup>22</sup> Anti-CTGF (rabbit, ab6992) and anti- $\beta$ -actin (rabbit, ab8227) antibodies were purchased from Abcam (Cambridge, UK). Anticardiac ventricular MLC (mouse, sc-517244), anti-ROCK1 (rabbit, sc-5560), and anti-ROCK2 (rabbit, sc-5561) antibodies were obtained from Santa Cruz Biotechnology (Dallas, TX). Anticardiac ventricular p-MLC (Ser 15, rabbit, PA5-104265) was obtained from Thermo Fisher Scientific (Waltham, MA). This was further probed with horseradish peroxidase-conjugated secondary antibody for 1 hour at room temperature, then washed in Tris-buffered saline containing 0.1% Tween 20. The membrane was stripped and reincubated with anti- $\beta$ -actin antibody (rabbit, 1:4000 dilution) for normalization. Chemiluminescence was performed for visualization using Amersham ECL and ECL Prime Western blotting detection reagent (GE Healthcare Life Sciences, Chicago, IL). Protein bands were obtained using FUSION Solo S (Vilber Lourmat, Paris, France), and signal densities were quantified using Image J software (version 1.49v, Wayne Rasband; National Institutes of Health, Bethesda, MD).

### Animal Preparation

All protocols were approved by the Institutional Animal Care and Use Committee of Mie University (protocol no. 30–11).

### Development of Mice With Conditional Knockout of Cardiac MLCP

Conditional targeting vector was constructed to delete a genomic fragment containing exon 3 of the *MYPT2* gene by homologous recombination (Figure S1). Two loxP sites flanking exon 3 were introduced. The neomycin resistance gene was inserted between exon 3 and the 3' loxP site. The 5' homology arm and the 3' homology arm were inserted upstream of the 5' loxP site and downstream of the 3' loxP site, respectively. The linearized targeting vector was injected into embryonic stem cells derived from SV/129 mice. Neomycin-resistant clones were screened for homologous recombination by genomic Southern blot. Correctly targeted clones were injected into C57BL/6 blastocysts. Male heterozygous MYPT2<sup>flox/flox</sup> mice were bred with C57BL/6 females to obtain heterozygous pups. Heterozygous mice were backcrossed to C57BL/6J for at least 7 generations. The  $\alpha$ MHC-MerCreMer mice were obtained from Jackson Laboratories (Bar Harbor, ME) and were originally generated by Dr Jeffrey Molkentin.<sup>26</sup> MYPT2-floxed mice were crossed with  $\alpha$ MHC-MerCreMer mice to obtain heterozygotes, which were injected intraperitoneally with tamoxifen (30  $\mu$ g/g, 3 consecutive days) at 8 weeks old to induce KO of MYPT2 in the heart. We decided the dose and timing of tamoxifen injection to prevent cardiac dysfunction due to tamoxifen-induced Cre,<sup>27,28</sup> by repeated trial and careful assessment of cardiac function by echo.

The MYPT2<sup>flox/flox</sup> mouse is available (R. Okamoto: ryuji@clin.medic.mie-u.ac.jp).

### MR-Related Hypertension Model

We used and defined an aldosterone-induced hypertension model that has been previously reported by Brilla et al<sup>29</sup> as an MR-related hypertension model in this study. Eight-week-old male cardiac-specific and inducible KO (c-MYPT2<sup>-/-</sup>) mice and their littermate MYPT2<sup>if/if</sup> (MYPT2<sup>+/+</sup>) mice were divided into the following groups (n=10 each): (c-MYPT2<sup>-/-</sup> control), MYPT2<sup>+/+</sup> control, c-MYPT2<sup>-/-</sup> MR-related hypertension (c-MYPT2<sup>-/-</sup>-Treated), and MYPT2<sup>+/+</sup> MR-related hypertension (MYPT2<sup>+/+</sup>-Treated). MR-related hypertension groups were uni-nephrectomized. After that, an osmotic minipump (model 1002; Alzet, Cupertino, CA) was implanted subcutaneously to infuse vehicle or aldosterone (0.15  $\mu$ g/h; Sigma-Aldrich, St. Louis, MO) in control or treated groups for 4 weeks, as previously

described.<sup>30,31</sup> Osmotic minipumps were replaced every 2 weeks. Heat support was provided throughout the procedure and during the recovery period. MR-related hypertension mice were fed a high-salt diet (8% NaCl), and control mice were fed a normal diet.

### Physiological Measurements

Noninvasive heart rate and tail-cuff blood pressure were measured weekly (BP-98AW; Softron Corp., Tokyo, Japan), as previously described.<sup>32</sup>

### Echocardiography

Transthoracic echocardiography was performed by observers blinded to the groups of the mice using the Vevo 2100 system (FUJIFILM VisualSonics, Toronto, Canada) with a 30-MHz transducer (MS-400; FUJIFILM VisualSonics) under 2% isoflurane gas anesthesia to assess cardiac function.<sup>33</sup> Mice were placed in the supine position on a heating pad to maintain body temperature. LV short-axis cross-sectional images (papillary muscle level) were visualized in M-mode.

### Speckle Tracking Echocardiography Measurements

Speckle tracking-based strain analysis of 3 consecutive cardiac cycles of 2-dimensional grayscale ECG images were acquired from parasternal long and short axes using the Vevostrain software package (FUJIFILM VisualSonics).<sup>34</sup> Endo- and epicardial borders were semiautomatically traced, then corrected as needed to achieve good quality throughout each cine cycle. Strain measurements were performed by processing tracking images in a frame-by-frame manner, then averaged from the acquired cardiac cycles, from which curve strain and strain rate data were obtained. The following were obtained from parasternal long-axis view analysis: (systolic global radial strain (GRS), systolic global longitudinal strain GLS, systolic GRS rate; systolic GLS rate, diastolic GRS rate, and diastolic GLS rate). All images were acquired at a frame rate >200 frames/s.

### Quantification of MLC Phosphorylation

Cardiac muscle that had been snap-frozen in liquid nitrogen was placed in a cold slurry of trichloroacetic acid (10% wt/vol) in acetone plus dithiothreitol (10 mmol/L) and triturated. Next, levels of MLC phosphorylation were measured as described previously, using an antibody specific for cardiac regulatory MLC (1:1000; Santa Cruz Biotechnology).<sup>15,20</sup> Immunostained proteins were visualized using the ECL plus (Sigma-Aldrich) method.

### Histology

Hearts were fixed in 4% paraformaldehyde, embedded in paraffin, and serially sectioned (2–3  $\mu$ m). Sections were stained with hematoxylin and eosin for histological examination of the myocardium or Masson trichrome for measurement of interstitial and perivascular fibrosis in the myocardium. All image analyses were conducted with an all-in-one fluorescence microscope (BZ-X710; Keyence Co.). LV myocardial cross-sectional area and cardiac interstitial fibrosis were measured as described elsewhere.<sup>33</sup> Approximately 30 to 40 cells or 15 fields were calculated per heart, then averages were used for analysis. Perivascular fibrosis was evaluated as the ratio of the area of fibrosis surrounding the vessel wall to the total vessel area, according to previous procedures.<sup>20,33</sup>

### Statistical Analysis

Statistical analyses were performed using SPSS version 20.0 software (IBM Inc., Chicago, IL). All experimental data were evaluated for normality by conducting formal normality tests (Shapiro–Wilk). Statistical significance was evaluated using Student's *t* test, 1-way ANOVA, or nonparametric tests followed by a least significant difference post hoc test. The paired Student's *t* test were used to compare pre- and posttreatment groups. The significance threshold was set at  $P < 0.05$ .

## RESULTS

### Aldosterone Increased Expressions of MYPT2 and CTGF With Decreased Phosphorylation of MLC in Cardiomyocytes

To examine the effects of aldosterone in the expression of CTGF and MLCP, we stimulated HL-1 cells as an established line of adult mouse cardiomyocytes and evaluated expressions of MLCP and CTGF. As MLCP consists of a catalytic subunit, PP1 $\beta$  (also known as PP1 $\delta$ ) and a regulatory subunit of MLCP, myosin phosphatase target subunit 2 (Figure 1A), MYPT2 was evaluated with CTGF. Aldosterone increased CTGF and MYPT2 in a dose-dependent manner from  $10^{-7}$  to  $10^{-5}$  mol/L in Figure 1B. The expression of PP1 $\beta$  was unchanged. On the other hand, cMLCK1 and 2,<sup>16</sup> counterparts of MLCP, were decreased in HL-1 cells after treatment of aldosterone (Figure 1B). Indeed, the level of MLC phosphorylation decreased according to the dose of aldosterone (Figure 1C). We evaluated the effects of aldosterone ( $10^{-6}$  mol/L) for 1 hour and 24 hours in HL-1 cell culture. Aldosterone significantly increased both CTGF and MYPT2 expression with 24 hours of incubation with the significant decrease in

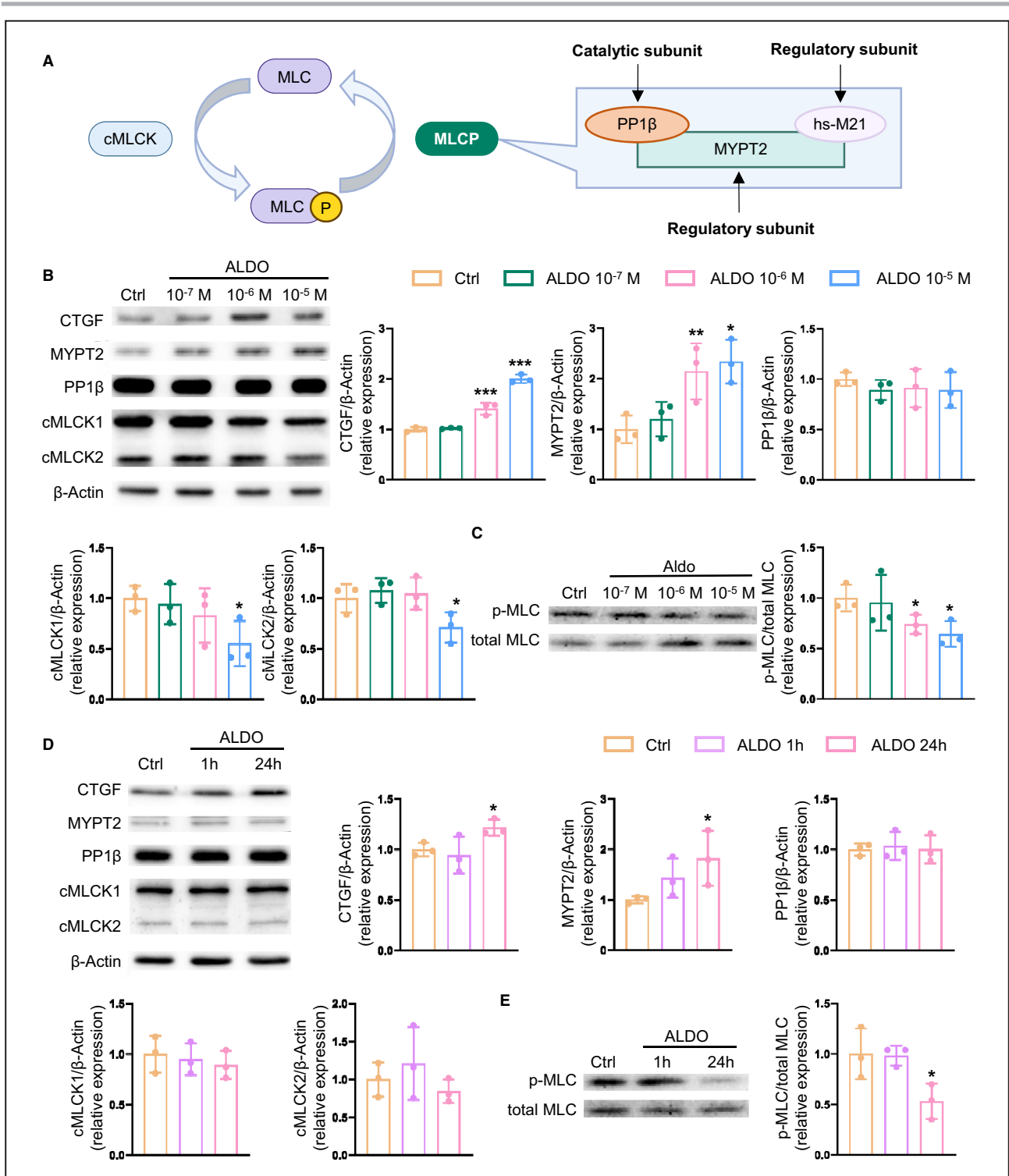


**Figure 1. Effect of aldosterone on the expression of connective tissue growth factor and myosin light chain phosphatase in cardiomyocytes.**

**A**, Regulation of MLC phosphorylation and structure of MLCP. **B** and **C**, Addition of different concentrations of aldosterone to HL-1 cardiomyocytes for 24 hours. Western blotting showed that aldosterone increased protein expression of CTGF and MYPT2, while decreasing cMLCK1, cMLCK2, and p-MLC in a dose-dependent manner. **D** and **E**, Effect of addition of  $10^{-6}$  mol/L aldosterone to HL-1 cardiomyocytes at different time points. Aldosterone increased CTGF and MYPT2, whereas decreased p-MLC (**E**) after treated for 24 hours ( $n=3$  per group).  $*P<0.05$ ;  $**P<0.01$ ;  $***P<0.001$  vs control. cMLCK indicates cardiac myosin light chain kinase; CTGF, connective tissue growth factor; hs-M21, heart-specific small regulatory subunit of myosin light chain phosphatase; MLC, myosin light chain; MLCP, myosin light chain phosphatase; MYPT, myosin phosphatase target subunit; p-MLC, phosphorylated myosin light chain; and PP1 $\beta$ , protein phosphatase catalytic subunit beta.

MLC phosphorylation (Figure 1D and 1E). No changes were observed in the expression of PP1 $\beta$  or cMLCK1 and 2 in HL-1 cells after treatment with aldosterone for 24 hours (Figure 1D).

Next, we investigated whether deletion of MYPT2 affects induction of CTGF in cardiomyocytes by aldosterone. We confirmed 2 kinds of siRNA of MYPT2 and knockdown 1 and 2 (Figure 2A and Data S1) in HL-1 cardiomyocytes and PP1 $\beta$  remained unchanged within 24 hours (Figure 2B). Interestingly, MYPT2-knockdown inhibited the increase in CTGF expression induced by aldosterone (Figure 2C). This was accompanied by an

increase in the level of phosphorylation of cardiac MLC (Figure 2D). Nuclear translocation of MR by aldosterone was not prevented by MYPT2-knockdown (Figure 2E).

### Cardiac-Specific Tamoxifen-Induced Loss of MLCP in c-MYPT2<sup>-/-</sup> Mice

To examine the effects of MLCP deletion in the heart, we developed mice with cardiomyocyte-specific deletion KO of MYPT2 (c-MYPT2<sup>-/-</sup> mice). At 8 weeks of age, c-MYPT2<sup>-/-</sup> mice were given tamoxifen to induce exon 3 excision from the floxed MYPT2 alleles

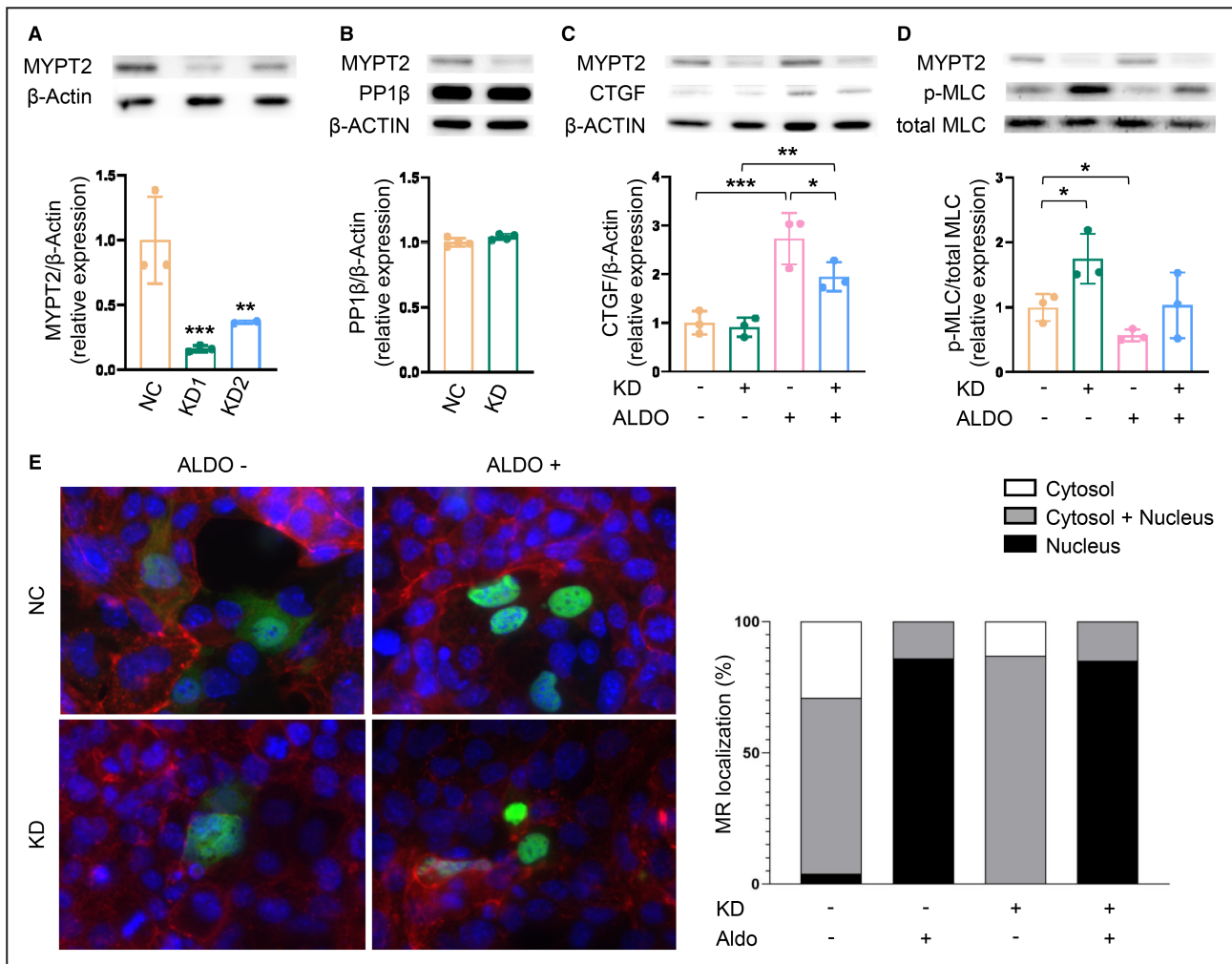


**Figure 2. Knockdown of MYPT2 suppressed the protein level of CTGF.**

**A,** Knockdown of MYPT2 with 2 different siRNAs was confirmed in HL-1 cardiomyocytes. **B,** No change in PP1 $\beta$  after knockdown of MYPT2. **C,** After incubation of aldosterone, knockdown of MYPT2 suppressed protein levels of CTGF compared with control cells. **D,** Incubation of aldosterone suppressed protein levels of p-MLC in control cells and knockdown of MYPT2 increased p-MLC in cells without aldosterone treatment (n=3 per group). **E,** Effects of aldosterone treatment and MYPT2 knockdown on subcellular localization of MR on HL-1 cardiomyocytes. Representative immunofluorescence staining of HL-1 transfected with human MR plasmid alone or in combination with MYPT2 siRNA, then treated with aldosterone or vehicle. MR stained green, F-Actin cytoskeleton stained red, and nuclei stained blue. MRs were mainly located in nuclei and cytoplasm before aldosterone treatment, and mainly in nuclei after aldosterone treatment. Knockdown of MYPT2 did not affect MR subcellular localization (60 cells per group). \* $P$ <0.05; \*\* $P$ <0.01; \*\*\* $P$ <0.001. CTGF indicates connective tissue growth factor; MLC, myosin light chain; MR, mineralocorticoid receptor; MYPT, myosin phosphatase target subunit; NC, negative control; p-MLC, phosphorylated myosin light chain; and PP1 $\beta$ , protein phosphatase catalytic subunit beta.

(Figure S1). One week later, assessment of MYPT2 protein levels from LV homogenates revealed a reduction of  $\approx 70\%$  in c-MYPT2<sup>-/-</sup> mice in comparison with MYPT2<sup>+/+</sup> mice (Figure 3A). We decided the dose and timing of tamoxifen injection to prevent cardiac dysfunction by tamoxifen-induced Cre with evaluation by cardiac echography. Expression levels of MYPT2 in the brain remained unchanged (data not shown). This was concomitant with significantly lower levels of the PP1 $\beta$  catalytic subunit of cardiac MLCP (Figure 3A). However, the third regulatory subunit (heart-specific small regulatory subunit of MLCP) and other MYPT family members including MYPT1 and myosin-binding subunit 85 were unchanged (Figure 3A). Further, cMLCK1 and cMLCK2 remained unchanged (Figure 3A). The level of MLC phosphorylation was significantly higher in c-MYPT2<sup>-/-</sup> mice than in MYPT2<sup>+/+</sup> mice (Figure 3B). Expression of ROCK, an important protein upstream of MYPT2, was unchanged in c-MYPT2<sup>-/-</sup> mice (Figure 3C). We confirmed that levels of TnI (troponin I) and PLB (phospholamban) phosphorylation were unaffected in c-MYPT2<sup>-/-</sup> mice (Figure S2 and Data S1), suggesting that cardiac MLC signaling does not extensively affect these signaling pathways.

### Cardiac Function Is Preserved in c-MYPT2<sup>-/-</sup> Mice With MR-Related Hypertension

The c-MYPT2<sup>-/-</sup> mice appeared normal, without any marked change in either appearance or behavior. Heart rate and blood pressures were not significantly altered in c-MYPT2<sup>-/-</sup> mice. The lifespan of this lineage was  $\approx 2$  years, almost the same as wild-type controls (Figure S3 and Data S1).

We further investigated the role of MYPT2 in a model of MR-related hypertension (Figure 4A). After 1 week of treatment, systolic blood pressure was significantly higher in the treated group than in the control group (Figure 4B). Cardiac deficiency of MYPT2 did not influence systolic blood pressure. The ratio of heart weight to body weight was significantly larger in treated mice than in control mice, as expected. Further, the ratio of tended to decrease after KO of MYPT2, but the difference was not significant (Figure 4C). The cross-sectional area of LV cardiomyocytes was similar in both groups with MR-related hypertension (Figure 4D). Interestingly, echocardiography showed significant increases in LV ejection fraction and fractional shortening, as well as a significant decrease in end-systolic LV diameter, were observed in c-MYPT2<sup>-/-</sup> mice with MR-related hypertension compared with MYPT2<sup>+/+</sup> mice (Table). The number of mice with ejection fraction lower than 50% was 7/10 and 3/10 in MYPT2<sup>+/+</sup> mice and c-MYPT2<sup>-/-</sup> mice (n=10, each) after treatment of aldosterone, respectively. This indicates that KO of MYPT2 did

not inhibit cardiac hypertrophy but maintained cardiac function to a certain extent in MR-related hypertension.

### Cardiac Fibrosis Is Inhibited in c-MYPT2<sup>-/-</sup> Mice With MR-Related Hypertension

Contrasting with the lack of observable differences in cardiac hypertrophy or nuclear translocation of MR by aldosterone (Figure S4 and Data S1) in c-MYPT2<sup>-/-</sup> and MYPT2<sup>+/+</sup> mice, a substantial difference in MR-related hypertension-induced increases in cardiac fibrosis was noted between c-MYPT2<sup>-/-</sup> and MYPT2<sup>+/+</sup> mice. Both cardiac interstitial and perivascular fibrosis were significantly reduced in c-MYPT2<sup>-/-</sup> mice compared with MYPT2<sup>+/+</sup> mice in the MR-related hypertension model (Figure 4E and 4F). We also further monitored transcript levels of CTGF, TGF- $\beta$  (transforming growth factor  $\beta$ ), periostin, atrial natriuretic factor, and BNP (brain natriuretic peptide). The results showed that periostin, atrial natriuretic factor, and BNP tended to be decreased in c-MYPT2<sup>-/-</sup> mice compared with MYPT2<sup>+/+</sup> mice in treated groups (Figure 5A), but the difference was not significant. However, CTGF was significantly reduced in c-MYPT2<sup>-/-</sup> mice with MR-related hypertension (Figure 5A). We speculate that c-MYPT2<sup>-/-</sup> mice achieve reduced fibrosis through the reduced expression of CTGF. Interestingly, MYPT2 expression was increased in MYPT2<sup>+/+</sup> mice after treatment with aldosterone (Figure 5B) and p-MLC was significantly decreased in c-MYPT2<sup>-/-</sup> mice compared with MYPT2<sup>+/+</sup> mice treated with aldosterone (Figure 5C). These results indicate that c-MYPT2<sup>-/-</sup> mice achieve attenuation of CTGF induction by aldosterone treatment (Figure 5; as shown in vivo in Figure 1).

### Higher Myocardial Strain Rate in c-MYPT2<sup>-/-</sup> Mice Before and After Aldosterone Treatment

Finally, we investigated myocardial strain in c-MYPT2<sup>-/-</sup> and MYPT2<sup>+/+</sup> mice, because cardiac MLC plays an important role in cardiac strain.<sup>35</sup> c-MYPT2<sup>-/-</sup> showed better GLS and GRS (systolic GLS and systolic GRS) before treatment with aldosterone (Figure 6A and 6B). After treatment with aldosterone for 28 days, both radial and longitudinal strain were reduced in both c-MYPT2<sup>-/-</sup> and MYPT2<sup>+/+</sup> mice, but systolic and diastolic GLS and GRS strain rates were still higher in c-MYPT2<sup>-/-</sup> mice compared with MYPT2<sup>+/+</sup> mice in Figure 6. In addition, ejection fraction and fractional shortening were significantly higher in c-MYPT2<sup>-/-</sup> mice compared with MYPT2<sup>+/+</sup> mice after treatment with aldosterone (Table). These results indicate that MYPT2 KO can prevent cardiac dysfunction in addition to cardiac fibrosis.

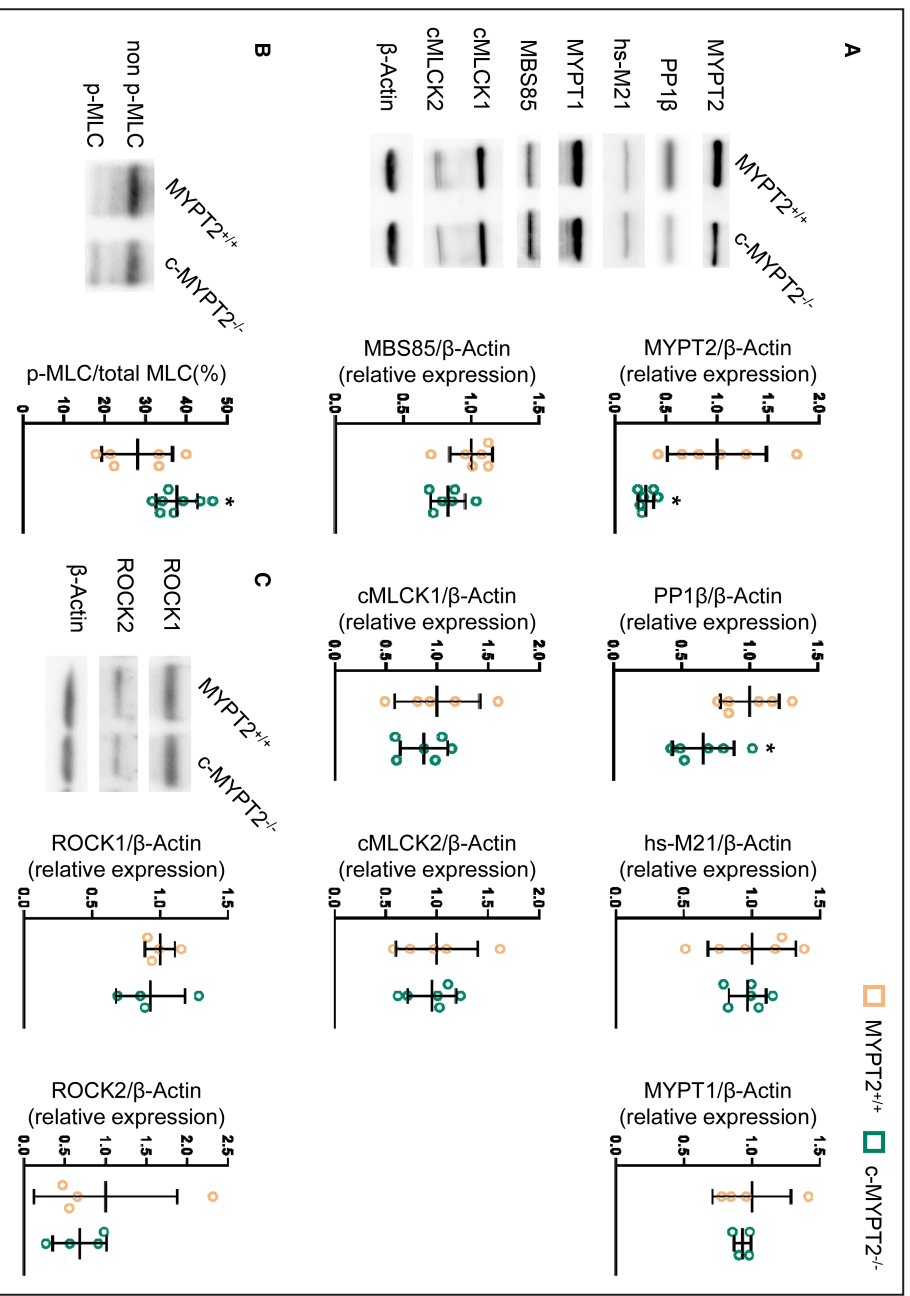


**Figure 3. Changes in protein levels in c-MYPT2<sup>-/-</sup> mice.**

**A**, Protein levels of MYPT2 expression in hearts from c-MYPT2<sup>-/-</sup> mice were decreased to <30% compared with MYPT2<sup>+/+</sup> mice. Protein levels of PP1β, as the catalytic subunit of cardiac MLC phosphatase, were decreased in c-MYPT2<sup>-/-</sup> mice compared with MYPT2<sup>+/+</sup> mice, while no changes were found in hs-M21, MYPT1, MBS85, or cMLCK1 or 2. **B**, The level of p-MLC was significantly higher in c-MYPT2<sup>-/-</sup> mice than in MYPT2<sup>+/+</sup> mice. **C**, No changes were found in ROCK1 or 2 (n=4–8 per group). \**P*<0.05 vs MYPT2<sup>+/+</sup> mice. cMLCK indicates cardiac myosin light chain kinase; c-MYPT2<sup>-/-</sup>, cardiac-specific inducible MYPT2-knockout; hs-M21, heart-specific small regulatory subunit of myosin light chain phosphatase; MBS85, myosin-binding subunit 85; MLC, myosin light chain; MYPT, myosin phosphatase target subunit; p-MLC, phosphorylated myosin light chain; PP1β, protein phosphatase catalytic subunit beta; and ROCK, Rho kinase.

## DISCUSSION

MR-related hypertension has recently been proposed to be associated with upregulation of Wnt5a-RhoA/ROCK-MYPT1 signaling in vascular smooth muscle cells.<sup>18,19</sup> However, whether this signaling represents the mechanism mediating cardiac hypertrophy and

fibrosis remains unknown. We discovered upregulation of MYPT2 and MLCp activity in cardiomyocytes both *in vivo* and *in vitro* after treatment with aldosterone. c-MYPT2<sup>-/-</sup> mice exhibited decreased cardiac fibrosis without attenuating cardiac hypertrophy in response to aldosterone. The mechanism partly involves increased levels of p-MLC and downregulation of CTGF in the

### Figure 4. Mice with cardiac-specific knockout of MYPT2 exhibited lower cardiac fibrosis.

**A**, Experimental design of the animal study. **B**, Elevation of blood pressure was observed in both mice with mineralocorticoid receptor-related hypertension (Treated group), whereas no change was evident between c-MYPT2<sup>-/-</sup> mice and MYPT2<sup>+/+</sup> mice (n=10 per group). \**P*<0.001 vs MYPT2<sup>+/+</sup>. Control; \**P*<0.001 vs c-MYPT2<sup>-/-</sup>. Control. **C**, No significant difference in heart size was found (n=12 per group). **D**, No significant difference in cardiomyocyte cross-sectional area was apparent between c-MYPT2<sup>-/-</sup> mice and MYPT2<sup>+/+</sup> mice (n=6 per group). **E**, **F**, Representative Masson's trichrome staining revealed that the degrees of interstitial fibrosis (**E**) and perivascular fibrosis (**F**) were lower in c-MYPT2<sup>-/-</sup> than in MYPT2<sup>+/+</sup> (n=6 per group). \**P*<0.05; \*\**P*<0.01; \*\*\**P*<0.001. BP indicates blood pressure; BW, body weight; c-MYPT2<sup>-/-</sup>, cardiac-specific MYPT2-knockout; HW, heart weight; MYPT, myosin phosphatase target subunit; qPCR, quantitative polymerase chain reaction; TAM, tamoxifen; Treated, mineralocorticoid receptor-related hypertension; and WB, Western blot.



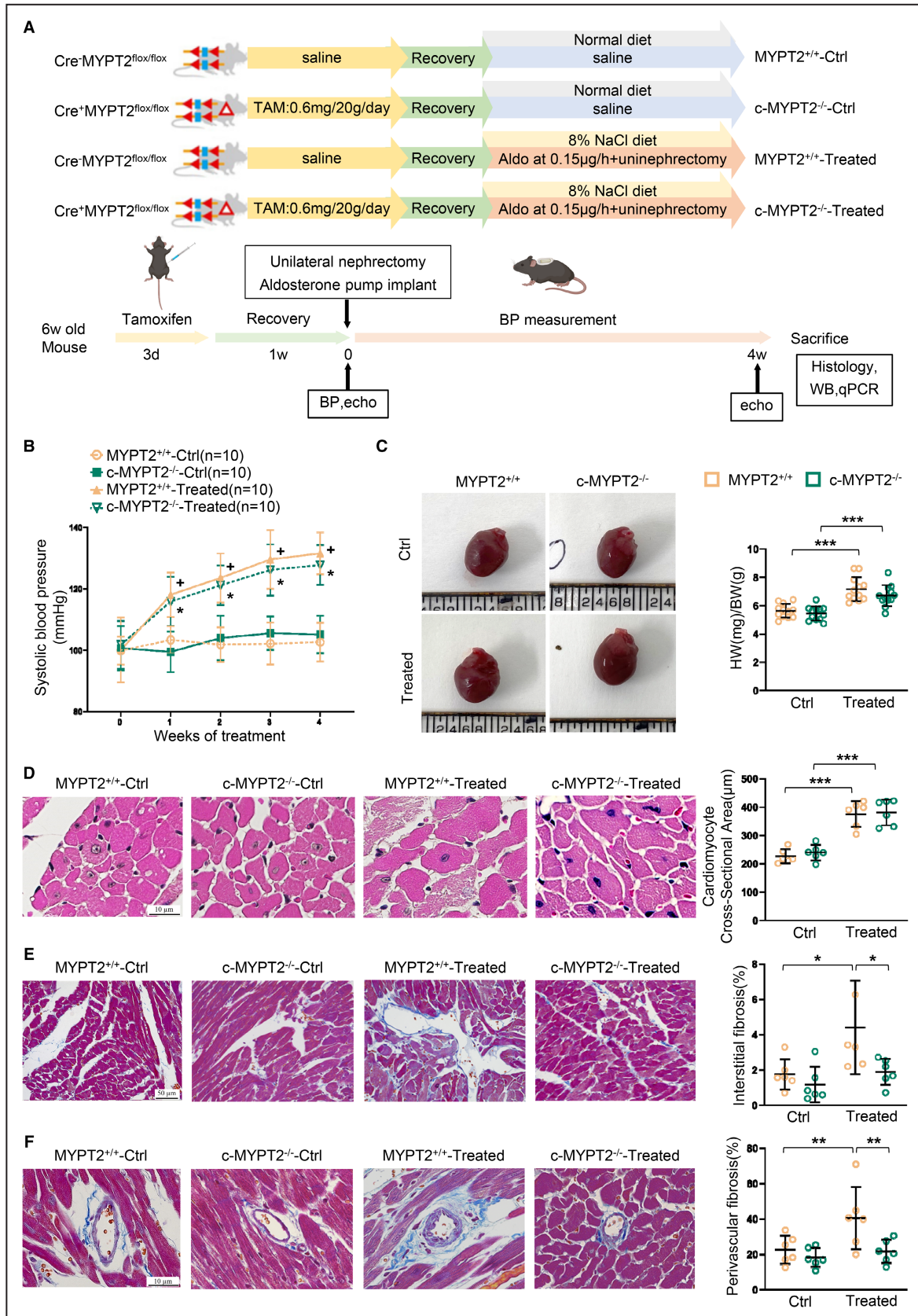


**Table. Changes in Hemodynamics of c-MYPT2<sup>-/-</sup> Mice and MYPT2<sup>+/+</sup> Mice Between Control and Mineralocorticoid Receptor-Associated Hypertension Groups**

	Control		Treated	
	MYPT2 <sup>+/+</sup> (n=10)	c-MYPT2 <sup>-/-</sup> (n=10)	MYPT2 <sup>+/+</sup> (n=10)	c-MYPT2 <sup>-/-</sup> (n=10)
IVST; d	0.85±0.11	0.85±0.09	0.82±0.11	0.90±0.15
IVST; s	1.22±0.21	1.33±0.15	1.11±0.17	1.25±0.23
LVD; d	3.73±0.38	3.93±0.18	4.19±0.37 <sup>†</sup>	3.97±0.44
LVD; s	2.58±0.28	2.64±0.26	3.13±0.37 <sup>†</sup>	2.80±0.45*
PWT; d	0.88±0.10	0.80±0.10	0.93±0.12	0.87±0.10
PWT; s	1.18±0.11	1.07±0.17	1.16±0.17	1.17±0.25
Ejection fraction, %	59.2±4.2	61.5±6.6	50.3±6.4 <sup>‡</sup> (39.3 to 62.4)	57.3±8.3* (43.9 to 66.2)
Fractional shortening, %	30.82±2.89	32.75±5.17	25.38±3.94 <sup>†</sup>	29.86±5.37*
LV mass	93.07±8.40	95.49±9.70	115.49±24.91 <sup>†</sup>	107.02±20.13
LV vol; d	60.01±14.19	67.29±6.97	78.88±15.99 <sup>†</sup>	70.04±18.12
LV vol; s	24.56±6.08	26.02±5.73	39.57±10.85 <sup>†</sup>	30.64±11.92

Values are mean±SD. c-MYPT2<sup>-/-</sup> indicates cardiac-specific MYPT2-knockout; d, diastole; IVST, interventricular septal wall thickness (mm); LVD, left ventricular dimension (mm); LVD, left ventricular dimension (mm); LV mass, left ventricle mass (mg); PWT, posterior wall thickness (mm); s, systole; and vol, volume (μL).

\*P<0.05 vs MYPT2<sup>+/+</sup>-treated.

<sup>†</sup>P<0.05.

<sup>‡</sup>P<0.01 vs MYPT2<sup>+/+</sup>-Control.

heart of c-MYPT2<sup>-/-</sup> mice (Figure 7). Interestingly, MYPT2 increased in response to aldosterone and KO of MYPT2 inhibited the upregulation of CTGF in mice and HL-1 cardiomyocytes accompanied by increased levels of p-MLC (Figure 7). The regulation of p-MLC levels has been proposed to mediate sarcomere organization without causing other aspects of the hypertrophic response, including cell size increases.<sup>36</sup> We could not find definitive differences in sarcomere length in cardiac tissue using anti- $\alpha$ -actinin immunostaining (data not shown). Rho/ROCK-MYPT signaling also appears to play an important role in cardiac fibrosis.<sup>37,38</sup> Further investigations are necessary to clarify the role of MLCP in both the heart and vasculature in MR-related hypertension using cardiac, endothelial, or smooth muscle-specific MLCP-deficient mice.

In c-MYPT2<sup>-/-</sup> mice, we could observe the downregulation of PP1 $\beta$  and no change in expression in cMLCK1 and 2 and other molecules related to cardiac MLC signaling. These results indicate that c-MYPT2<sup>-/-</sup> mice function as MLCP complex-deficient mice and no other molecules are able to compensate for this deficiency.

The phosphorylation level of a protein is given by the balance between the activities of protein kinases and protein phosphatases. The degree of ventricular p-MLC2 is mainly determined by the balance between cMLCK and MLCP. Hitsumoto et al discovered a decreased mRNA expression ratio of *MYLK3/PPP1R12B*, the encoding gene of cMLCK and MYPT2, in human myocardium with advanced heart failure compared with control hearts.<sup>39</sup> Here, we

confirmed this at the protein level, aldosterone stimulation of HL-1 cells resulted in increased MYPT2 expression and decreased cMLCK expression, resulting in a reduced cMLCK/MYPT2 protein ratio compared with controls. This suggests that aldosterone may play a role in modulating the balance of cMLCK and MLCP in failing myocardium.

We found that MYPT2 was increased and p-MLC was decreased after treatment with aldosterone in mice and HL-1 cells. These results were partly inconsistent with findings from previous reports. Aoki et al reported skeletal MLCK expression and levels of MLC phosphorylation were increased in rat neonatal cardiomyocytes after stimulation with angiotensin II and endothelin. When their study was performed, in 2000, skeletal MLCK was thought to be the same as cMLCK.<sup>36</sup> Correct identification of cMLCK was not achieved until Takashima and Kitakaze's group discovered in 2007 that this was the most increased molecule in explanted hearts from patients with dilated cardiomyopathy receiving heart transplant.<sup>40,41</sup> Whether increased or decreased phosphorylation level of MLC is better for the heart in patients with heart disease has remained contentious. Indeed, transgenic mice overexpressing MLCP, showing decreased levels of MLC phosphorylation, demonstrate dilated cardiomyopathy in the natural course.<sup>15</sup> In addition, C57BL/6N, a mouse line naturally deficient in cMLCK1 with decreased levels of p-MLC that was discovered independently by our laboratory<sup>16</sup> and other groups, can develop mild dilated cardiomyopathy in the natural aging process.<sup>17</sup> Furthermore, cMLCK mutation is 1 reason for familial dilated

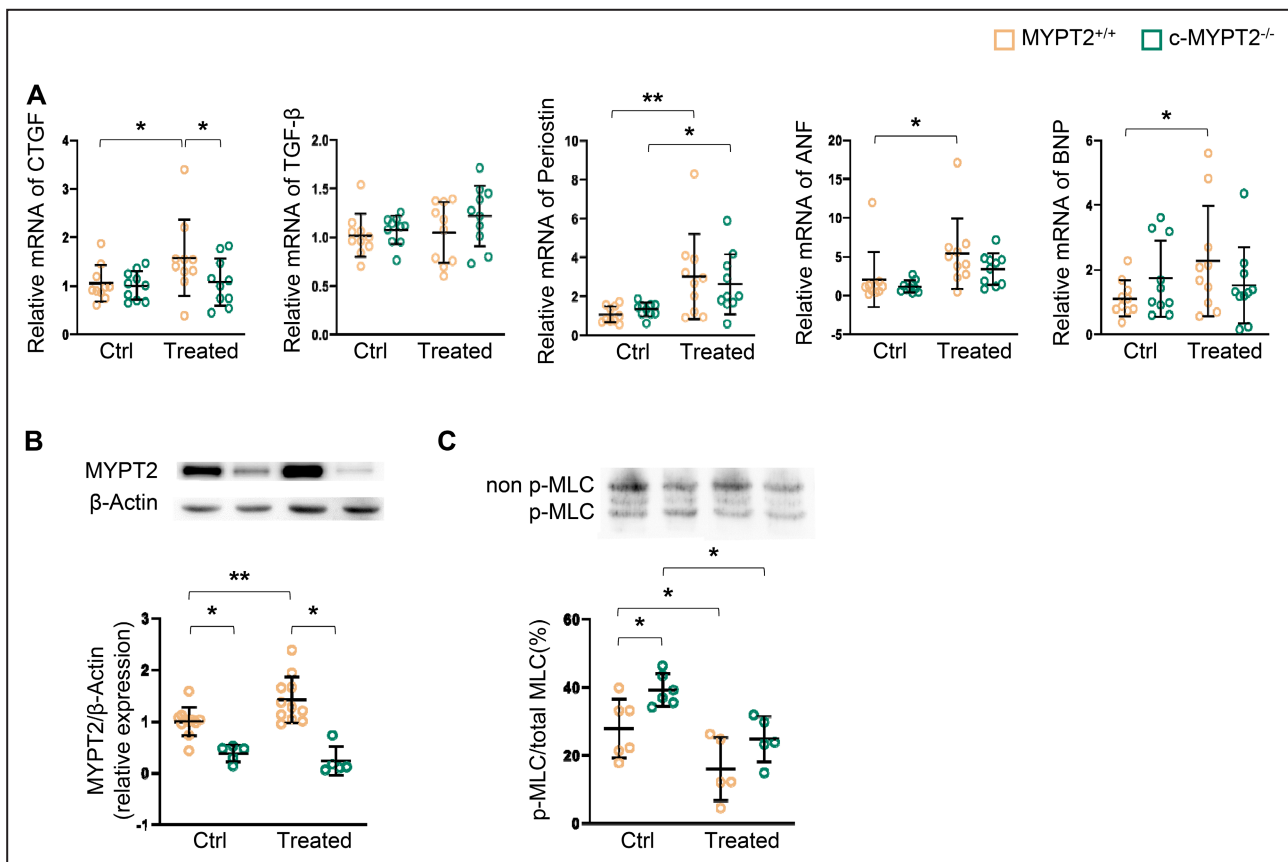


**Figure 5. MYPT2 knockout can relieve cardiac fibrosis.**

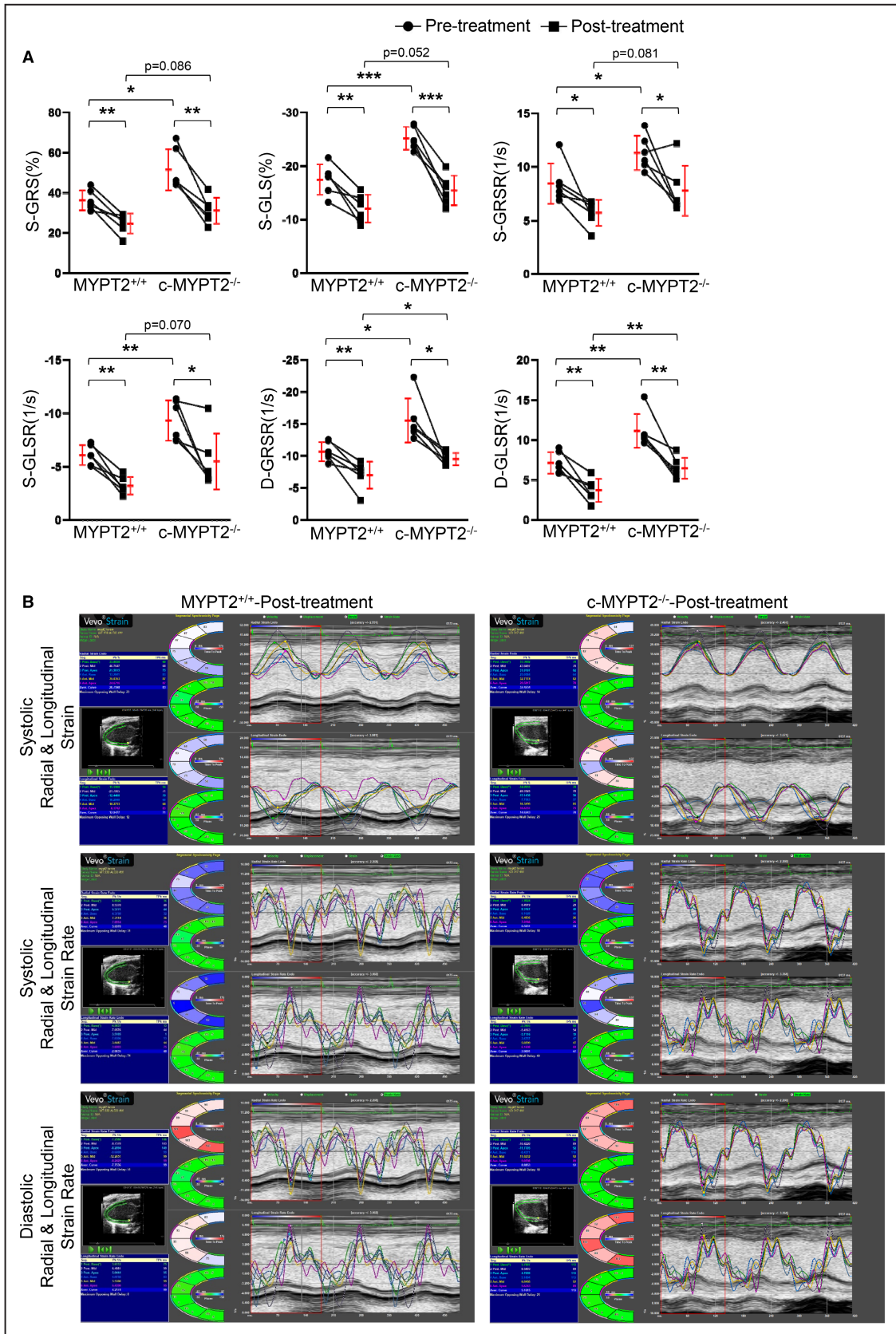
**A**, The mRNA levels of *CTGF*, *periostin*, *ANF*, and *BNP* were significantly higher in the MR-related hypertension group than in the control group of MYPT2<sup>+/+</sup> mice. The mRNA levels of *periostin* was significantly higher in the MR-related hypertension group than in the control group, while no changes were found in TGF-β. The mRNA levels of *CTGF* were significantly lower in c-MYPT2<sup>-/-</sup> mice than in MYPT2<sup>+/+</sup> mice with MR-related hypertension (n=10 per group). **B**, MYPT2 was increased in MYPT2<sup>+/+</sup>-Treated mice with aldosterone compared with MYPT2<sup>+/+</sup>-Control mice (n=5–11 per group). **C**, Urea gel analysis showed levels of phosphorylation in MLC in different groups (n=5–6 per group). ANF indicates atrial natriuretic factor; BNP, brain natriuretic peptide; CTGF, connective tissue growth factor; MLC, myosin light chain; MYPT, myosin phosphatase target subunit; p-MLC, phosphorylated myosin light chain; TGF, transforming growth factor; and Treated, mineralocorticoid receptor-related hypertension.

cardiomyopathy with decreased p-MLC<sup>13,14</sup> and cardiac MLC mutation is 1 reason for midventricular-type hypertrophic cardiomyopathy.<sup>42</sup> Adenoviral cMLCK expression and an activator of cMLCK have very recently been shown to improve systolic dysfunction in mice and cardiomyocytes via increases in p-MLC levels.<sup>39</sup> On the other hand, Rho kinase inhibitors and ROCK-deficient mouse models also show protective effects with decreased level of p-MLC.<sup>22,43,44</sup> Interestingly, TRV 120023, a beta-arresting-biased ligand, has been reported to increase the phosphorylation of MLC<sup>45</sup> and inhibit angiotensin II-induced hypertrophy while preserving enhanced myofilament response to calcium.<sup>46</sup> Interestingly, in end-stage human heart failure, the level of p-MLC was decreased, although the calcium sensitivity was enhanced.<sup>12</sup> On the other hand, increased p-MLC has been reported in compensatory adaptive phase of human heart failure.<sup>47</sup> These conflicting lines of evidence indicate that regulation of the p-MLC level

needs fine-tuning in both rodents and humans, dependent on timing, duration, and organ-specificity.

Crosstalk between p-MLC and phosphorylation of TnI is also interesting, because these signaling pathways play important roles in cardiac contraction and calcium sensitivity, and sometimes compensate for each other.<sup>48</sup> In end-stage human heart failure, the p-MLC level and not the p-TnI level is significantly lower than in donors.<sup>12</sup> We observed that levels of TnI phosphorylation were unchanged in c-MYPT2<sup>-/-</sup> mice (Figure S2), as cMLCK can phosphorylate human but not rodent TnI.<sup>49</sup> The phosphatase that dephosphorylates TnI has yet to be identified.

Speckle tracking echocardiography with myocardial strain and strain rate is a more sensitive method to detect initial changes in the heart and can identify subtle adaptive changes in LV contractile mechanics in hypertensive patients without symptoms or signs of heart failure and with normal contractile function.<sup>50,51</sup> Myocardial



Downloaded from <http://ahajournals.org> by on March 11, 2024

**Figure 6. MYPT2 knockout can prevent cardiac dysfunction.**

**A**, Global strain and strain rate analyses in the parasternal long-axis view (n=5 per group). **B**, Representative systolic radial and longitudinal strain, strain rate and diastolic radial and longitudinal strain rate images for each group. \* $P < 0.05$ ; \*\* $P < 0.01$ ; \*\*\* $P < 0.001$ . D-GLSR indicates diastolic global longitudinal strain rate; D-GRSR, diastolic global radial strain rate; MYPT, myosin phosphatase target subunit; S-GLS, systolic global longitudinal strain; S-GLSR, systolic global longitudinal strain rate; S-GRS, systolic global radial strain; and S-GRSR, systolic global radial strain rate.

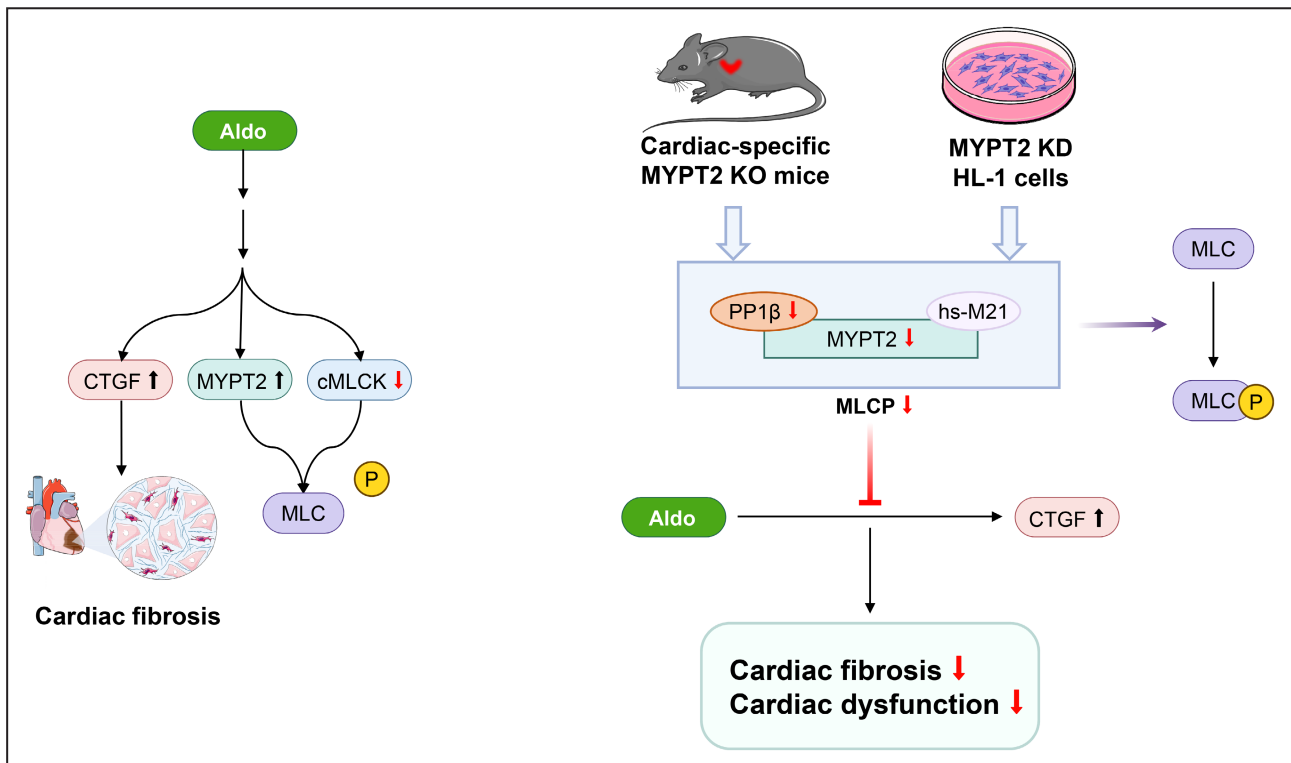
strain and strain rate are also more sensitive to early and subtle changes in rodent cardiac function.<sup>52</sup> In this study, although conventional echocardiography did not show any difference between c-MYPT2<sup>-/-</sup> and MYPT2<sup>+/+</sup> mice at baseline, speckle tracking echocardiography showed that radial and longitudinal strain and strain rate were higher in c-MYPT2<sup>-/-</sup> mice than in MYPT2<sup>+/+</sup> mice. Because p-PLB and p-Tnl were unchanged, we suggest that this might be partly due to upregulation of p-MLC via loss of MYPT2. After aldosterone treatment, c-MYPT2<sup>-/-</sup> mice showed higher ejection fraction and fractional shortening compared with MYPT2<sup>+/+</sup> mice. This further demonstrates that MYPT2-deficient mice exhibit enhanced cardiac contractility. Further investigations are necessary to investigate to clarify whether this higher strain and strain rate at the basal level in c-MYPT2<sup>-/-</sup> mice can contribute to the prevention of

cardiac fibrosis or dysfunction in other MR-related and non-MR-mediated hypertension model.

CTGF plays an important role in the development of cardiac fibrosis. Originally, agonists including TGF- $\beta$ , angiotensin II, and vascular endothelial growth factor were thought to be capable of inducing CTGF expression. Recently, CTGF expression has been reported to be sensitive to mechanical strain via the involvement of Rho.<sup>10</sup> MYPT2 is a downstream target of the Rho-ROCK pathway.<sup>22</sup> As a result, MYPT2 deficiency could plausibly contribute to decreases in CTGF expression by indirectly inhibiting Rho signaling.

**Limitations**

In this paper, we did not investigate whether aldosterone directly or indirectly increased MYPT2. We also did

**Figure 7. Summary of current study findings.**

The mechanism of action of aldosterone and the cardioprotective effect of MYPT2. Parts of the figure were drawn by using pictures from Servier Medical Art. Servier Medical Art by Servier is licensed under a Creative Commons Attribution 3.0 Unported License (<https://creativecommons.org/licenses/by/3.0/>). cMLCK indicates cardiac myosin light chain kinase; CTGF, connective tissue growth factor; hs-M21, heart-specific small regulatory subunit of myosin light chain phosphatase; KO, cardiac-specific knockout; MLC, myosin light chain; MLCP, myosin light chain phosphatase; MYPT, myosin phosphatase target subunit; and PP1 $\beta$ , protein phosphatase catalytic subunit beta.

not investigate whether this is mediated by the MR or not. Further investigations including other hypertensive models and the site of genetic manipulation of MR are necessary to make these clear.

## CONCLUSIONS

Our findings suggest that MYPT2 is an important therapeutic target for preventing cardiac fibrosis in a model of MR-related hypertension. However, further studies are required to clarify how MYPT2 deletion leads to inhibited upregulation of CTGF and whether Rho/ROCK-MLCP plays an important role in the transition from cardiac fibrosis to heart failure or arrhythmia in MR-related hypertension.

## ARTICLE INFORMATION

Received September 26, 2023; accepted January 24, 2024.

### Affiliations

Department of Cardiology and Nephrology, Mie University Graduate School of Medicine, Tsu, Mie, Japan (Z.Y., R.O., H.I., R.I., K.M., M.I., L.K., M.I., K.D.); Regional Medical Support Center, Mie University Hospital, Tsu, Mie, Japan (R.O.); Department of Clinical Training and Career Support Center, Mie University Hospital, Tsu, Mie, Japan (R.O.); and Department of Pharmacology and Toxicology, University of Mississippi Medical Center, Jackson, MS (Y.A., C.E.G.).

### Sources of Funding

This work was supported in part by Grants-in-Aid for Scientific Research from the Ministry of Education, Culture, Sports, Science and Technology, Japan (no. 19K08578 and no. 22K08098 to R.O.).

### Disclosures

Dr Dohi reports research grants from Bristol-Myers Squibb, MSD K.K., Pfizer Japan Inc., Takeda Pharmaceutical Co., Ltd., Astellas Pharma Inc., Daiichi Sankyo Pharmaceutical Co., Ltd., Genzyme Japan, Shionogi & Co., Ltd., Sumitomo Dainippon Pharma Co., Ltd., Mitsubishi Tanabe Corporation, Otsuka Pharmaceutical Co., Ltd., Bayer Yakuhin, Ltd., AstraZeneca K.K., and Boehringer Ingelheim Co., Ltd. These funders played no roles in the design or conduct of the study, in the collection, analysis, or interpretation of the data, or in the preparation, review, or approval of the article. The remaining authors have no disclosures to report.

### Supplemental Material

Data S1.

Figures S1–S4.

References<sup>53,54</sup>

## REFERENCES

- Ferrario CM, Schiffrin EL. Role of mineralocorticoid receptor antagonists in cardiovascular disease. *Circ Res*. 2015;116:206–213. doi: [10.1161/CIRCRESAHA.116.302706](https://doi.org/10.1161/CIRCRESAHA.116.302706)
- Rossi GP. Primary aldosteronism: JACC state-of-the-art review. *J Am Coll Cardiol*. 2019;74:2799–2811. doi: [10.1016/j.jacc.2019.09.057](https://doi.org/10.1016/j.jacc.2019.09.057)
- Monticone S, D'Ascenzo F, Moretti C, Williams TA, Veglio F, Gaita F, Mulatero P. Cardiovascular events and target organ damage in primary aldosteronism compared with essential hypertension: a systematic review and meta-analysis. *Lancet Diabetes Endocrinol*. 2018;6:41–50. doi: [10.1016/S2213-8587\(17\)30319-4](https://doi.org/10.1016/S2213-8587(17)30319-4)
- Freel EM, Mark PB, Weir RA, McQuarrie EP, Allan K, Dargie HJ, McClure JD, Jardine AG, Davies E, Connell JM. Demonstration of blood pressure-independent noninfarct myocardial fibrosis in primary aldosteronism: a

- cardiac magnetic resonance imaging study. *Circ Cardiovasc Imaging*. 2012;5:740–747. doi: [10.1161/CIRCIMAGING.112.974576](https://doi.org/10.1161/CIRCIMAGING.112.974576)
- Tsai CH, Pan CT, Chang YY, Chen ZW, Wu VC, Hung CS, Lin YH. Left ventricular remodeling and dysfunction in primary aldosteronism. *J Hum Hypertens*. 2021;35:131–147. doi: [10.1038/s41371-020-00426-y](https://doi.org/10.1038/s41371-020-00426-y)
- Rossi GP, Sacchetto A, Pavan E, Palatini P, Graniero GR, Canali C, Pessina AC. Remodeling of the left ventricle in primary aldosteronism due to Conn's adenoma. *Circulation*. 1997;95:1471–1478. doi: [10.1161/01.cir.95.6.1471](https://doi.org/10.1161/01.cir.95.6.1471)
- Stehr CB, Mellado R, Ocaranza MP, Carvajal CA, Mosso L, Becerra E, Solis M, Garcia L, Lavandero S, Jalil J, et al. Increased levels of oxidative stress, subclinical inflammation, and myocardial fibrosis markers in primary aldosteronism patients. *J Hypertens*. 2010;28:2120–2126. doi: [10.1097/HJH.0b013e328333d0177](https://doi.org/10.1097/HJH.0b013e328333d0177)
- Edelman ER, Butala NM, Avery LL, Lundquist AL, Dighe AS. Case 30-2020: a 54-year-old man with sudden cardiac arrest. *N Engl J Med*. 2020;383:1263–1275. doi: [10.1056/NEJMcp2002420](https://doi.org/10.1056/NEJMcp2002420)
- Dorn LE, Petrosino JM, Wright P, Accornero F. CTGF/CCN2 is an autocrine regulator of cardiac fibrosis. *J Mol Cell Cardiol*. 2018;121:205–211. doi: [10.1016/j.yjmcc.2018.07.130](https://doi.org/10.1016/j.yjmcc.2018.07.130)
- Cicha I, Goppelt-Struebe M. Connective tissue growth factor: context-dependent functions and mechanisms of regulation. *Biofactors*. 2009;35:200–208. doi: [10.1002/biof.30](https://doi.org/10.1002/biof.30)
- Ito M, Okamoto R, Ito H, Zhe Y, Dohi K. Regulation of myosin light-chain phosphorylation and its roles in cardiovascular physiology and pathophysiology. *Hypertens Res*. 2022;45:40–52. doi: [10.1038/s41440-021-00733-y](https://doi.org/10.1038/s41440-021-00733-y)
- van der Velden J, Papp Z, Zaremba R, Boontje NM, de Jong JW, Owen VJ, Burton PB, Goldmann P, Jaquet K, Stienen GJ. Increased Ca<sup>2+</sup>-sensitivity of the contractile apparatus in end-stage human heart failure results from altered phosphorylation of contractile proteins. *Cardiovasc Res*. 2003;57:37–47. doi: [10.1016/s0008-6363\(02\)00606-5](https://doi.org/10.1016/s0008-6363(02)00606-5)
- Tobita T, Nomura S, Morita H, Ko T, Fujita T, Toko H, Uto K, Hagiwara N, Aburatani H, Komuro I. Identification of MYLK3 mutations in familial dilated cardiomyopathy. *Sci Rep*. 2017;7:17495. doi: [10.1038/s41598-017-17769-1](https://doi.org/10.1038/s41598-017-17769-1)
- Hodatsu A, Fujino N, Uyama Y, Tsukamoto O, Imai-Okazaki A, Yamazaki S, Seguchi O, Konno T, Hayashi K, Kawashiri MA, et al. Impact of cardiac myosin light chain kinase gene mutation on development of dilated cardiomyopathy. *ESC Heart Fail*. 2019;6:406–415. doi: [10.1002/ehf2.12410](https://doi.org/10.1002/ehf2.12410)
- Mizutani H, Okamoto R, Moriki N, Konishi K, Taniguchi M, Fujita S, Dohi K, Onishi K, Suzuki N, Satoh S, et al. Overexpression of myosin phosphatase reduces Ca<sup>2+</sup> sensitivity of contraction and impairs cardiac function. *Circ J*. 2010;74:120–128. doi: [10.1253/circj.cj-09-0462](https://doi.org/10.1253/circj.cj-09-0462)
- Taniguchi M, Okamoto R, Ito M, Goto I, Fujita S, Konishi K, Mizutani H, Dohi K, Hartshorne DJ, Itoh T. New isoform of cardiac myosin light chain kinase and the role of cardiac myosin phosphorylation in alpha1-adrenoceptor mediated inotropic response. *PLoS One*. 2015;10:e0141130. doi: [10.1371/journal.pone.0141130](https://doi.org/10.1371/journal.pone.0141130)
- Williams JL, Paudyal A, Awad S, Nicholson J, Grzesik D, Botta J, Meimaridou E, Maharaj AV, Stewart M, Tinker A, et al. Mylk3 null C57BL/6N mice develop cardiomyopathy, whereas Nnt null C57BL/6J mice do not. *Life Sci Alliance*. 2020;3:e201900593. doi: [10.26508/lsa.201900593](https://doi.org/10.26508/lsa.201900593)
- Kawarazaki W, Mizuno R, Nishimoto M, Ayuzawa N, Hirohama D, Ueda K, Kawakami-Mori F, Oba S, Marumo T, Fujita T. Salt causes aging-associated hypertension via vascular Wnt5a under klotho deficiency. *J Clin Invest*. 2020;130:4152–4166. doi: [10.1172/JCI134431](https://doi.org/10.1172/JCI134431)
- Fujita T. Recent advances in hypertension: epigenetic mechanism involved in development of salt-sensitive hypertension. *Hypertension*. 2023;80:711–718. doi: [10.1161/HYPERTENSIONAHA.122.20588](https://doi.org/10.1161/HYPERTENSIONAHA.122.20588)
- Okamoto R, Li Y, Noma K, Hiroi Y, Liu PY, Taniguchi M, Ito M, Liao JK. FHL2 prevents cardiac hypertrophy in mice with cardiac-specific deletion of ROCK2. *FASEB J*. 2013;27:1439–1449. doi: [10.1096/fj.12-217018](https://doi.org/10.1096/fj.12-217018)
- Surks HK, Mochizuki N, Kasai Y, Georgescu SP, Tang KM, Ito M, Lincoln TM, Mendelsohn ME. Regulation of myosin phosphatase by a specific interaction with cGMP-dependent protein kinase Ialpha. *Science*. 1999;286:1583–1587. doi: [10.1126/science.286.5444.1583](https://doi.org/10.1126/science.286.5444.1583)
- Okamoto R, Kato T, Mizoguchi A, Takahashi N, Nakakuki T, Mizutani H, Isaka N, Imanaka-Yoshida K, Kaibuchi K, Lu Z, et al. Characterization and function of MYPT2, a target subunit of myosin phosphatase in heart. *Cell Signal*. 2006;18:1408–1416. doi: [10.1016/j.cellsig.2005.11.001](https://doi.org/10.1016/j.cellsig.2005.11.001)

23. Robert V, Silvestre JS, Charlemagne D, Sabri A, Trouve P, Wassef M, Swynghedauw B, Delcayre C. Biological determinants of aldosterone-induced cardiac fibrosis in rats. *Hypertension*. 1995;26:971–978. doi: [10.1161/01.hyp.26.6.971](https://doi.org/10.1161/01.hyp.26.6.971)
24. Claycomb WC, Lanson NA Jr, Stallworth BS, Egeland DB, Delcarpio JB, Bahinski A, Izzo NJ Jr. HL-1 cells: a cardiac muscle cell line that contracts and retains phenotypic characteristics of the adult cardiomyocyte. *Proc Natl Acad Sci USA*. 1998;95:2979–2984. doi: [10.1073/pnas.95.6.2979](https://doi.org/10.1073/pnas.95.6.2979)
25. Shimizu H, Ito M, Miyahara M, Ichikawa K, Okubo S, Konishi T, Naka M, Tanaka T, Hirano K, Hartshorne DJ, et al. Characterization of the myosin-binding subunit of smooth muscle myosin phosphatase. *J Biol Chem*. 1994;269:30407–30411. doi: [10.1016/S0021-9258\(18\)43828-8](https://doi.org/10.1016/S0021-9258(18)43828-8)
26. Sohal DS, Nghiem M, Crackower MA, Witt SA, Kimball TR, Tymitz KM, Penninger JM, Molkenin JD. Temporally regulated and tissue-specific gene manipulations in the adult and embryonic heart using a tamoxifen-inducible Cre protein. *Circ Res*. 2001;89:20–25. doi: [10.1161/hh1301.092687](https://doi.org/10.1161/hh1301.092687)
27. Bersell K, Choudhury S, Molloy M, Polizzotti BD, Ganapathy B, Walsh S, Wadugu B, Arab S, Kuhn B. Moderate and high amounts of tamoxifen in alphaMHC-MerCreMer mice induce a DNA damage response, leading to heart failure and death. *Dis Model Mech*. 2013;6:1459–1469. doi: [10.1242/dmm.010447](https://doi.org/10.1242/dmm.010447)
28. Hall ME, Smith G, Hall JE, Stec DE. Systolic dysfunction in cardiac-specific ligand-inducible MerCreMer transgenic mice. *Am J Physiol Heart Circ Physiol*. 2011;301:H253–H260. doi: [10.1152/ajpheart.00786.2010](https://doi.org/10.1152/ajpheart.00786.2010)
29. Brilla CG, Pick R, Tan LB, Janicki JS, Weber KT. Remodeling of the rat right and left ventricles in experimental hypertension. *Circ Res*. 1990;67:1355–1364. doi: [10.1161/01.res.67.6.1355](https://doi.org/10.1161/01.res.67.6.1355)
30. Sawada H, Naito Y, Oboshi M, Iwasaku T, Okuhara Y, Morisawa D, Eguchi A, Hirotsu S, Masuyama T. Iron restriction inhibits renal injury in aldosterone/salt-induced hypertensive mice. *Hypertension Res*. 2015;38:317–322. doi: [10.1038/hr.2015.13](https://doi.org/10.1038/hr.2015.13)
31. Kagiya S, Matsumura K, Goto K, Otsubo T, Iida M. Role of rho kinase and oxidative stress in cardiac fibrosis induced by aldosterone and salt in angiotensin type 1a receptor knockout mice. *Regul Pept*. 2010;160:133–139. doi: [10.1016/j.regpep.2009.12.002](https://doi.org/10.1016/j.regpep.2009.12.002)
32. Ali Y, Dohi K, Okamoto R, Katayama K, Ito M. Novel molecular mechanisms in the inhibition of adrenal aldosterone synthesis: action of tolvaptan via vasopressin V(2) receptor-independent pathway. *Br J Pharmacol*. 2019;176:1315–1327. doi: [10.1111/bph.14630](https://doi.org/10.1111/bph.14630)
33. Ito H, Okamoto R, Ali Y, Zhe Y, Katayama K, Ito M, Dohi K. Cardiorenal protective effects of sodium-glucose cotransporter 2 inhibition in combination with angiotensin II type 1 receptor blockade in salt-sensitive dahl rats. *J Hypertens*. 2022;40:956–968. doi: [10.1097/HJH.0000000000003099](https://doi.org/10.1097/HJH.0000000000003099)
34. Zhang TY, Zhao BJ, Wang T, Wang J. Effect of aging and sex on cardiovascular structure and function in wildtype mice assessed with echocardiography. *Sci Rep*. 2021;11:22800. doi: [10.1038/s41598-021-02196-0](https://doi.org/10.1038/s41598-021-02196-0)
35. Davis JS, Hassanzadeh S, Winitsky S, Lin H, Satorius C, Vemuri R, Aletras AH, Wen H, Epstein ND. The overall pattern of cardiac contraction depends on a spatial gradient of myosin regulatory light chain phosphorylation. *Cell*. 2001;107:631–641. doi: [10.1016/S0092-8674\(01\)00586-4](https://doi.org/10.1016/S0092-8674(01)00586-4)
36. Aoki H, Sadoshima J, Izumo S. Myosin light chain kinase mediates sarcomere organization during cardiac hypertrophy in vitro. *Nat Med*. 2000;6:183–188. doi: [10.1038/72287](https://doi.org/10.1038/72287)
37. Rikitake Y, Liao JK. Rho-kinase mediates hyperglycemia-induced plasminogen activator inhibitor-1 expression in vascular endothelial cells. *Circulation*. 2005;111:3261–3268. doi: [10.1161/CIRCULATIONAHA.105.534024](https://doi.org/10.1161/CIRCULATIONAHA.105.534024)
38. Zhang YM, Bo J, Taffet GE, Chang J, Shi J, Reddy AK, Michael LH, Schneider MD, Entman ML, Schwartz RJ, et al. Targeted deletion of ROCK1 protects the heart against pressure overload by inhibiting reactive fibrosis. *FASEB J*. 2006;20:916–925. doi: [10.1096/fj.05-5129com](https://doi.org/10.1096/fj.05-5129com)
39. Hitsumoto T, Tsukamoto O, Matsuoka K, Li J, Liu L, Kuramoto Y, Higo S, Ogawa S, Fujino N, Yoshida S, et al. Restoration of cardiac myosin light chain kinase ameliorates systolic dysfunction by reducing superrelaxed myosin. *Circulation*. 2023;147:1902–1918. doi: [10.1161/CIRCULATIONAHA.122.062885](https://doi.org/10.1161/CIRCULATIONAHA.122.062885)
40. Seguchi O, Takashima S, Yamazaki S, Asakura M, Asano Y, Shintani Y, Weinberg EO, Aoki H, Sato N, Chien KR, et al. Identification of cardiac-specific myosin light chain kinase regulates sarcomere assembly in the vertebrate heart. *J Clin Invest*. 2007;117:2812–2824. doi: [10.1172/JCI30804](https://doi.org/10.1172/JCI30804)
41. Chan JY, Takeda M, Briggs LE, Graham ML, Lu JT, Horikoshi N, Weinberg EO, Aoki H, Sato N, Chien KR, et al. Identification of cardiac-specific myosin light chain kinase. *Circ Res*. 2008;102:571–580. doi: [10.1161/CIRCRESAHA.107.161687](https://doi.org/10.1161/CIRCRESAHA.107.161687)
42. Sheikh F, Lyon RC, Chen J. Functions of myosin light chain-2 (MYL2) in cardiac muscle and disease. *Gene*. 2015;569:14–20. doi: [10.1016/j.gene.2015.06.027](https://doi.org/10.1016/j.gene.2015.06.027)
43. Hattori T, Shimokawa H, Higashi M, Hiroki J, Mukai Y, Tsutsui H, Kaibuchi K, Takeshita A. Long-term inhibition of rho-kinase suppresses left ventricular remodeling after myocardial infarction in mice. *Circulation*. 2004;109:2234–2239. doi: [10.1161/01.CIR.0000127939.16111.58](https://doi.org/10.1161/01.CIR.0000127939.16111.58)
44. Rikitake Y, Oyama N, Wang CY, Noma K, Satoh M, Kim HH, Liao JK. Decreased perivascular fibrosis but not cardiac hypertrophy in ROCK1+/- haploinsufficient mice. *Circulation*. 2005;112:2959–2965. doi: [10.1161/CIRCULATIONAHA.105.584623](https://doi.org/10.1161/CIRCULATIONAHA.105.584623)
45. Tarigopula M, Davis RT III, Mungai PT, Ryba DM, Wiecek DF, Cowan CL, Violin JD, Wolska BM, Solaro RJ. Cardiac myosin light chain phosphorylation and inotropic effects of a biased ligand, TRV120023, in a dilated cardiomyopathy model. *Cardiovasc Res*. 2015;107:226–234. doi: [10.1093/cvr/cvv162](https://doi.org/10.1093/cvr/cvv162)
46. Monasky MM, Taglieri DM, Henze M, Warren CM, Utter MS, Soergel DG, Violin JD, Solaro RJ. The beta-arrestin-biased ligand TRV120023 inhibits angiotensin II-induced cardiac hypertrophy while preserving enhanced myofilament response to calcium. *Am J Physiol Heart Circ Physiol*. 2013;305:H856–H866. doi: [10.1152/ajpheart.00327.2013](https://doi.org/10.1152/ajpheart.00327.2013)
47. Toepfer C, Caorsi V, Kampourakis T, Sikkil MB, West TG, Leung MC, Al-Saud SA, MacLeod KT, Lyon AR, Marston SB, et al. Myosin regulatory light chain (RLC) phosphorylation change as a modulator of cardiac muscle contraction in disease. *J Biol Chem*. 2013;288:13446–13454. doi: [10.1074/jbc.M113.455444](https://doi.org/10.1074/jbc.M113.455444)
48. Sheikh F, Lyon RC, Chen J. Getting the skinny on thick filament regulation in cardiac muscle biology and disease. *Trends Cardiovasc Med*. 2014;24:133–141. doi: [10.1016/j.tcm.2013.07.004](https://doi.org/10.1016/j.tcm.2013.07.004)
49. Sevrieva IR, Brandmeier B, Ponnamm S, Gautel M, Irving M, Campbell KS, Sun YB, Kampourakis T. Cardiac myosin regulatory light chain kinase modulates cardiac contractility by phosphorylating both myosin regulatory light chain and troponin I. *J Biol Chem*. 2020;295:4398–4410. doi: [10.1074/jbc.RA119.011945](https://doi.org/10.1074/jbc.RA119.011945)
50. Tadic M, Cuspidi C, Marwick TH. Phenotyping the hypertensive heart. *Eur Heart J*. 2022;43:3794–3810. doi: [10.1093/eurheartj/ehac393](https://doi.org/10.1093/eurheartj/ehac393)
51. Oh JK, Park JH. Role of strain echocardiography in patients with hypertension. *Clin Hypertens*. 2022;28:6. doi: [10.1186/s40885-021-00186-y](https://doi.org/10.1186/s40885-021-00186-y)
52. Qi Y, Chen Z, Guo B, Liu Z, Wang L, Liu S, Xue L, Ma M, Yin Y, Li Y, et al. Speckle-tracking echocardiography provides sensitive measurements of subtle early alterations associated with cardiac dysfunction in T2DM rats. *BMC Cardiovasc Disord*. 2023;23:266. doi: [10.1186/s12872-023-03239-2](https://doi.org/10.1186/s12872-023-03239-2)
53. Okamoto R, Goto I, Nishimura Y, Kobayashi I, Hashizume R, Yoshida Y, Ito R, Kobayashi Y, Nishikawa M, Ali Y, et al. Gap junction protein beta 4 plays an important role in cardiac function in humans, rodents, and zebrafish. *PLoS One*. 2020;15:e0240129. doi: [10.1371/journal.pone.0240129](https://doi.org/10.1371/journal.pone.0240129)
54. Gomez-Sanchez CE, de Rodriguez AF, Romero DG, Estess J, Warden MP, Gomez-Sanchez MT, Gomez-Sanchez EP. Development of a panel of monoclonal antibodies against the mineralocorticoid receptor. *Endocrinology*. 2006;147:1343–1348. doi: [10.1210/en.2005-0860](https://doi.org/10.1210/en.2005-0860)

# **Supplemental Material**



## **Data S1.**

### **Supplemental Methods**

Anti-troponin I (rabbit, 4002) and anti-phospho-troponin I (Ser23/24, rabbit, 4004) were obtained from Cell Signaling Technology (Danvers, MA, USA). Anti-phospholamban (mouse, MA3-922) was from Invitrogen (Waltham, MA, USA) and phospho-phospholamban (Ser16, rabbit, 07-052) was from Merck Millipore.

### **Transfection of HL-1 cardiomyocytes**

Two different small interfering RNAs of MYPT2 (siMYPT2#1, s116360; siMYPT2#2, s116362) and one siRNA of the universal negative control were designed and synthesized by Thermo Fisher Scientific for transient silencing in HL-1 cells. Transient transfection was performed using Lipofectamine RNAiMAX Reagent (Thermo Fisher Scientific). Twenty-four hours after transfection, cells were changed to medium with or without  $10^{-6}$  mol/L Aldo. After cultivation for 24 h, cells were harvested and extracted protein was subjected to Western blotting analysis.

### **Immunofluorescence microscopy**

After transfection with siMYPT2 or universal negative control siRNA for 24 h, HL-1 cells were

co-transfected with hMR plasmid (RC220558; OriGene Technologies, Rockville, MD, USA) by Lipofectamine 3000 (Thermo Fisher Scientific) for 24 h. Cells were then transferred to serum-free medium for 24 h of serum starvation. Cells were subsequently treated with Aldo ( $10^{-6}$  mol/L) or vehicle for 1 h. Immunofluorescence microscopy was performed essentially as previously described<sup>53</sup>. MR was detected with previously characterized monoclonal antibodies<sup>54</sup>. The secondary antibody was Alexa-488 goat anti-mouse immunoglobulin G (Thermo Fisher Scientific). Nuclei were counterstained using diamidino-2-phenylindole. For the visualization of the actin fibers, rhodamine-phalloidin (Cytoskeleton, Denver, CO, USA) were used. Fluorescent images were acquired with an all-in-one fluorescence microscope (BZ-X710; Keyence Co., Osaka, Japan). Cells were classified into three classes based on the subcellular localization of MR. At least 60 cells were scored for each group. Data are presented as the percentage of cells in each category compared to the total number of scored cells.

### **Immunohistochemical analysis of MR localization in mice hearts**

Paraffin-embedded sections were deparaffinized in xylene, hydrated in a graded alcohol series, and washed in phosphate-buffered saline (PBS). Deparaffinized sections were heated for 5 min in citrate buffer at 100°C with a pressure cooker to reactivate the antigen, then treated with 0.3% H<sub>2</sub>O<sub>2</sub> for 30 min to abolish endogenous peroxidase activity. The Vector M.O.M. immunodetection kit (PK-2200; Vector Laboratories, Burlingame, CA, USA) was then used in accordance with the

instructions from the manufacturer. MR was detected with a 1:100 dilution of monoclonal antibody against rMR 1-18(6G1) as previously described<sup>54</sup>. PBS was used as a negative control to reveal any background staining.

### **Real-time PCR**

Total RNA was extracted from mice heart apices using the RNeasy Mini Kit (Qiagen, Hilden, Germany) according to the protocol from the manufacturer. An equal amount of RNA was reverse-transcribed to obtain the cDNA template using the SuperScript II RT (Thermo Fisher Scientific) following the protocol from the manufacturer. Real-time PCR was performed using a 7300 Real-Time PCR System (Thermo Fisher Scientific). Amplification was performed with the following time course: preincubation at 50°C for 2 min, 95°C for 10 min, and 40 cycles of 95°C for 15 s, 60°C for 60 s. Levels of mRNA were normalized to levels of the GAPDH housekeeping gene. TaqMan probe sets for mouse CTGF (Mm01178820\_m1), transforming growth factor beta (TGF)- $\beta$  (Mm01178820\_m1), periostin (Mm01284919\_m1), brain natriuretic peptide (BNP) (Mm00435304\_g1), atrial natriuretic factor (ANF) (Mm01255747\_g1), and GAPDH (Mm99999915\_g1) were purchased from Thermo Fisher Scientific.

### **PCR genotyping of MYPT2**

PCR genotyping of MYPT2 was performed using the following primers: forward primer,

CTTCCCTTTGTTGAGATTACAGGT; reverse primer, TTCTTGGTTAGGTTTCTTACCTCAA.

PCR product sizes are 237 and 800 base pairs for the floxed and wild-type alleles, respectively.

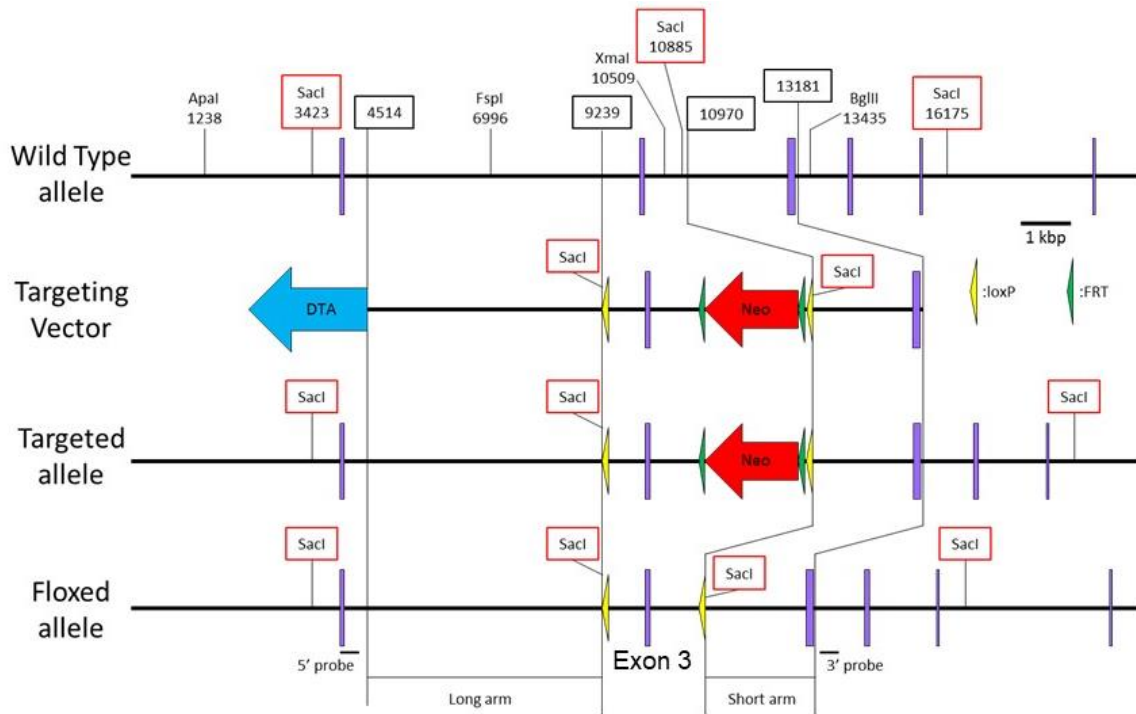
PCR genotyping of  $\alpha$ MHC-MerCreMer was performed using the following primers: forward primer, CTGAAAAGTTAACCAGGTGAGAATG; reverse primer,

AGGTAGTTATTCGGATCATCAGCTA. PCR product size is 2.2 kilobase pairs for the transgenic allele.

PCR genotyping of null MYPT2 was performed using the following primers: forward primer, TGAAA ACTAAAAGATGCTGGTAAGG; reverse primer, AACTGTAGTCCTATGGGATCTGATG.

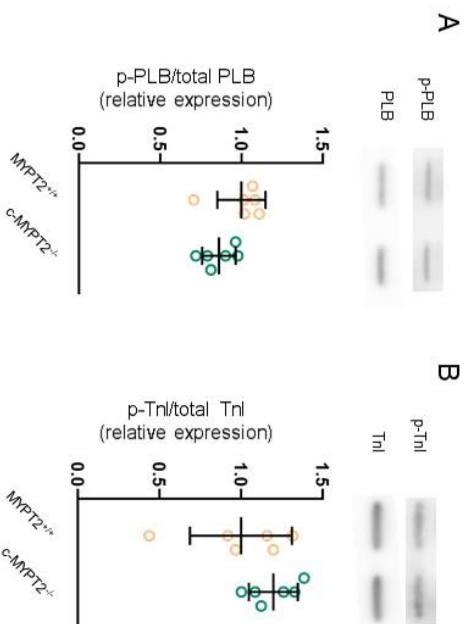
PCR product sizes are 910 and 2,553 base pairs for the floxed and wild-type alleles, respectively.

**Figure S1. Targeting strategy by homologous recombination of myosin phosphatase target subunit 2 (MYPT2).**



Structures of the wild-type allele (top row), gene targeting vector (middle row) and targeted allele (bottom row) are shown. DT-A, diphtheria toxin-A cassette; FRT, flippase recognition target site; loxP, locus of X(cross)-over in P1 site; Neo, neomycin cassette. Floxed mice were generated after excision of Neo by crossing with FLP transgenic mice. The floxed allele has no Neo or FRT.

**Figure S2. Changes in protein levels in cardiac-specific inducible knockout mice.**

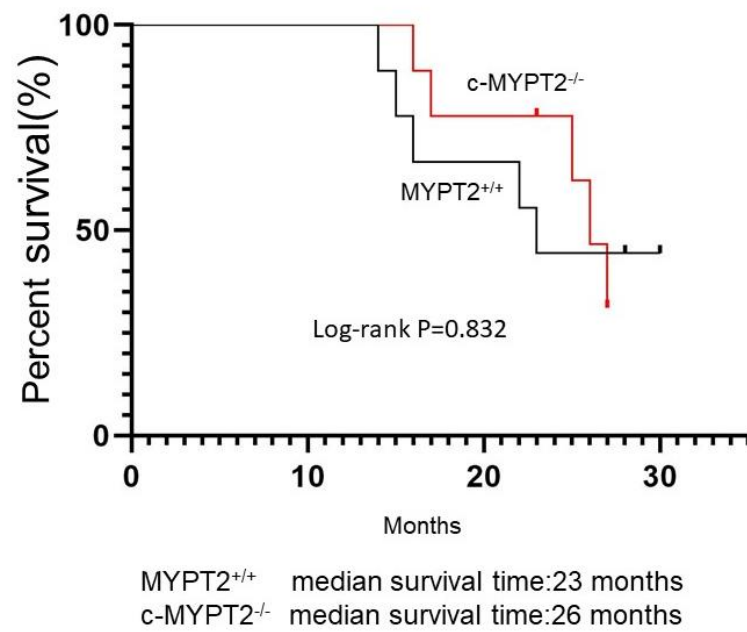


**A)** Phosphorylation (Ser16) and expression of phospholamban (PLB) (n=4/group).

**B)** Phosphorylation (Ser23/24) and expression of troponin I (TnI) (n=4/group).

MYP2, myosin phosphatase target subunit.

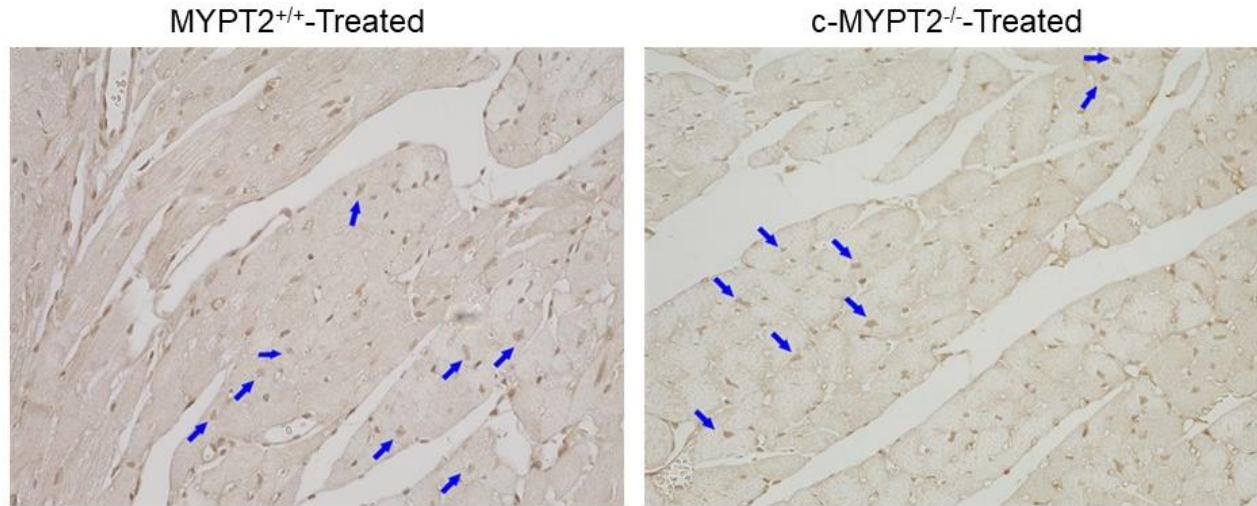
**Figure S3. Survival curves in cardiac-specific and inducible knockout (c-MYPT2<sup>-/-</sup>) mice and littermate MYPT2<sup>f/f</sup> (MYPT2<sup>+/+</sup>) mice.**



Median survival time tended to be longer in c-MYPT2<sup>-/-</sup> female mice (26 months) than in MYPT2<sup>+/+</sup> female mice (23 months), but the difference was not significant (n=9/group).

MYPT, myosin phosphatase target subunit.

**Figure S4. Immunohistochemical analysis of MR localization in mouse heart sections.**



Representative micrographs from mouse heart sections show exclusive nuclear mineralocorticoid receptor (MR) staining (arrows) in both MYPT2<sup>+/+</sup>-Treated and c-MYPT2<sup>-/-</sup>-Treated mice with aldosterone. MYPT, myosin phosphatase target subunit.